AWARD NUMBER:     W81XWH-10-1-0774


TITLE:   Theory-Driven Models for Correcting "Fight or Flight" Imbalance in Gulf War Illness


PRINCIPAL INVESTIGATOR:   Gordon Broderick, Ph.D.


CONTRACTING ORGANIZATION:        University of Alberta
                                                            Edmonton,  Alberta, Canada  T6G 2C8


REPORT DATE:     September 2012


TYPE OF REPORT:    Annual


PREPARED FOR:   U.S. Army Medical Research and Materiel Command
                               Fort Detrick, Maryland  21702-5012


DISTRIBUTION STATEMENT: Approved for Public Release;
                                            Distribution Unlimited

# REPORT DOCUMENTATION PAGE

*Form Approved*
*OMB No. 0704-0188*

Public reporting burden for this collection of information is estimated to average 1 hour per response, including the time for reviewing instructions, searching existing data sources, gathering and maintaining the data needed, and completing and reviewing this collection of information. Send comments regarding this burden estimate or any other aspect of this collection of information, including suggestions for reducing this burden to Department of Defense, Washington Headquarters Services, Directorate for Information Operations and Reports (0704-0188), 1215 Jefferson Davis Highway, Suite 1204, Arlington, VA 22202-4302. Respondents should be aware that notwithstanding any other provision of law, no person shall be subject to any penalty for failing to comply with a collection of information if it does not display a currently valid OMB control number. **PLEASE DO NOT RETURN YOUR FORM TO THE ABOVE ADDRESS.**

| 1. REPORT DATE | 2. REPORT TYPE | 3. DATES COVERED |
|---|---|---|
| 1 September 2012 | Annual | 1 Sep 2011 – 31 Aug 2012 |

| 4. TITLE AND SUBTITLE | 5a. CONTRACT NUMBER |
|---|---|
| Theory-Driven Models for Correcting "Fight or Flight" Imbalance in Gulf War Illness | |
| | 5b. GRANT NUMBER |
| | W81XWH-10-1-0774 |
| | 5c. PROGRAM ELEMENT NUMBER |

| 6. AUTHOR(S) | 5d. PROJECT NUMBER |
|---|---|
| Gordon Broderick, P.hD. | |
| | 5e. TASK NUMBER |
| Email: gordon.broderick@ualberta.ca | 5f. WORK UNIT NUMBER |

| 7. PERFORMING ORGANIZATION NAME(S) AND ADDRESS(ES) | 8. PERFORMING ORGANIZATION REPORT NUMBER |
|---|---|
| University of Alberta<br>Edmonton, Alberta, Canada T6G 2C8 | |

| 9. SPONSORING / MONITORING AGENCY NAME(S) AND ADDRESS(ES) | 10. SPONSOR/MONITOR'S ACRONYM(S) |
|---|---|
| U.S. Army Medical Research and Materiel Command<br>Fort Detrick, Maryland 21702-5012 | |
| | 11. SPONSOR/MONITOR'S REPORT NUMBER(S) |

**12. DISTRIBUTION / AVAILABILITY STATEMENT**
Approved for Public Release; Distribution Unlimited

**13. SUPPLEMENTARY NOTES**

**14. ABSTRACT**
The objective of this study is to create a comprehensive engineering model of endocrine-immune interaction dynamics in order to identify (i) theoretical failure modes of the HPA-immune axis that align with GWI, and (ii) promising treatment strategies that exploit the regulatory dynamics of these systems to reset control of the HPA-immune axis to normal. We recruited a new senior research associate, Dr. Craddock, effective January 1, 2012. Work has begun in earnest and we have completed a first detailed model of immune circuitry as well as a broader model describing the interplay of the HPA axis with the immune and sex hormone (HPG) axes in both male and female subjects. Alignment of these models was evaluated against experimental data from veterans (Dr. Klimas; Miami VA). The significant overlap of the latter with predicted homeostatic states is consistent with the chronic nature of this illness.

**15. SUBJECT TERMS**
GWI; Hypothalamic-pituitary-adrenal (HPA) axis

| 16. SECURITY CLASSIFICATION OF: | | | 17. LIMITATION OF ABSTRACT | 18. NUMBER OF PAGES | 19a. NAME OF RESPONSIBLE PERSON USAMRMC |
|---|---|---|---|---|---|
| a. REPORT | b. ABSTRACT | c. THIS PAGE | UU | 73 | 19b. TELEPHONE NUMBER (include area code) |
| U | U | U | | | |

**Standard Form 298 (Rev. 8-98)**
**Prescribed by ANSI Std. Z39.18**

**Table of Contents**

## Introduction

The hypothalamic-pituitary-adrenal (HPA) axis controls the body's "fight or flight" response through a series of endocrine and immune signals directed at ensuring immediate survival and later re-establishing homeostasis. Changes in the tone of this response have been observed in veterans with Gulf War Illness (GWI). Studies report abnormal cell proliferation, impaired function and persistent oxidative stress in circulating immune cells of patients. Similarly dysregulation of the HPA axis includes hypersensitivity in cytokine feedback as well as suppression of cortisol and neurotransmitters responsible for mediating innate and adaptive immunity. This is further complicated by the impact on the HPA axis of a myriad of regulatory interactions both within and between i) the immune system and ii) the sex-hormone axis, the hypothalamic-pituitary-gonadal (HPG) axis.

We proposed that severe physical or psychological insult to the endocrine and immune systems can displace these from a normal regulatory equilibrium into a compromised stable state. This state is characterized by a self-perpetuating inflammatory response that involves regulatory imbalance between the HPA, HPG and immune axes. To explore the validity of this hypothesis our objective was to create comprehensive engineering models of endocrine-immune interaction dynamics in order to identify (i) theoretical failure modes of the endocrine-immune interplay that align with GWI, and (ii) promising treatment strategies that exploit the naturally occurring stable points of these systems.

## Body.

At the time of our last update we had initiated work consistent with Task 3 in the original Statement of Work (SOW). This analysis had focused mainly on the recovery and re-assessment of the basic differential equation model for the HPA axis reported in Ben-Zvi et al., 2009 [1]. We identified a number of shortcomings in this basic model. In particular, we assessed the natural frequencies supported by the basic model and found the latter did not naturally support circadian rhythm without an external forcing function. In addition, analysis of limited experimental data in female subjects with a closely related illness, chronic fatigue syndrome (CFS) [2], suggested that a linear model of the adrenal gland might be limited in terms of fidelity. The apparent need for increased dynamic complexity created an important challenge to the continued use of conventional differential equation modeling, as significant gaps in the required parameter estimates exist in the literature. To circumvent this problem we critically re-assessed our approach. Rather than rely on questionable estimates of dynamic parameters we have shifted our approach to one that exploits a much larger body of information, namely known physiological and biochemical connectivity. The approach is inspired from circuit theory and is described below. *Importantly, this approach supports the seamless integration of kinetic information wherever available, be it simple sequential precedence, relative time scale or detailed dynamics*. This shift in paradigm, together with the concerted efforts of Dr. Craddock who joined in January of this year, has allowed us to continue moving forward on Task 3 and make substantial progress on Task 2, 4 and 5 of the SOW with the added help of Mr. Paul Fritsch (research intern).

1.      *Re-assessment and adaptation of modeling paradigm (**Task 1**)*. The core concept of the approach we have used is *connectivity*. There is a substantial body of anatomical and biochemical data for many biological systems describing the connectivity between components, however data regarding the precise stoichiometry and kinetics of these interactions in humans is extremely limited. Existing models rely heavily on animal data as a source of kinetic parameters, or adopt general order of magnitude estimates when this data is lacking. To circumvent this issue and draw on this rich body of physiological and biochemical wiring diagrams, we have adopted the discrete logical network methodology proposed originally by Thomas et al. [3,4] and developed further by Mendoza and Xenarios [5]. Analysis of these networks makes it possible to identify the number and type (e.g. oscillatory, etc...) of resting states as well as their molecular and cellular profile without detailed knowledge of response dynamics. We have used this methodology to construct 2 complementary models at different scales.

2.      *An integrated model of HPA-HPG-immune interaction (**Task 3, Task 5**)*. Here we extended our previous analysis of HPA axis dynamics [1] by including feed-forward and feedback interactions with sex

hormone regulation and immune response. A circuit model was constructed that linked state variables across the HPA axis with hypothalamic-pituitary-gonadal (HPG) function in both men and women, as well as innate (IIR) and adaptive (AIR) immune response. The latter was described by the expression of specific subsets of cytokines. Details of this analysis are described in Appendix A in the form of a completed manuscript that is currently under internal review by collaborating co-authors [6]. In brief, interactions between the HPA, HPG and immune systems were described as a circuit model consisting of 11 state variable nodes where each node can assume one of three states at any point in time: -1 (inhibited), 0 (nominal) and +1 (elevated). In this model the HPA axis was described by 5 state-variable nodes: corticotropin-releasing hormone (CRH), adrenocorticotropic hormone (ACTH), cortisol (CORT) and cytostolic glucocorticoid receptors (GRs), which unlike membrane bound receptors, dimerize (GRD). As a first coarse model, immune function was described in terms of innate immune response (IIR) and adaptive immune response (AIR). The state of activation of the IIR node was meant to capture changes in cytokines produced by the innate response including the pro-inflammatory cytokines interleukin (IL) 1, 6, 8 and tumor necrosis factor alpha (TNF-α). Also represented by the IIR node were IL-12 and IL-15, two mediators of NK cell function, as well as IL-23, an important inflammatory signal contributing to the Th17 response. Cytokines represented by the AIR node include IL-2, IL-4, IL-5, IL-13, interferon-gamma (IFN-γ), and TNF-β. As IL-10 is produced by both the IIR and AIR, it was represented as a separate state-variable node. HPG function was described by the levels of gonadotropin-releasing hormone (GnRH), of luteinizing homone (LH) as well as testosterone (TEST) in males (Figure 1A) and estradiol (EST) in females (Figure 1B). The effects of gender merit special attention. While testosterone (TEST) exhibits an inhibitory effect on all levels of the HPA axis, estrogen (EST) and progesterone can stimulate or suppress HPA activity depending on the phase of menstrual cycle.  It remains unclear whether this inhibition/stimulation of the HPA axis occurs in concert with the inhibition/stimulation of the HPG.  As a result, these cases were explored as separate alternative models of the HPA-HPG interaction in female subjects.

In this formalism, the overall state of the system is described by a vector of discrete values, either -1, 0 or +1, expressed at each state-variable node (Eq. 1). This evolves over time and at each time step the next state value $x_i(t+1)$ for the $i^{th}$ node in the system is determined from that node's current state as well as a set of balanced ternary logic statements based on the state values of the neighboring input nodes and their mode of action (i.e. activate or inhibit). The logic statements that determine a state transition are expressed as follows (Eq. 2-4):

$$\vec{x}(t) = (x_1(t), x_2(t)...x_N(t)) \tag{1}$$

$$x_i(t+1) = \begin{cases} (x_{i1}^A(t) \vee x_{i2}^A(t)...\vee x_{ij}^A(t)) \lozenge (x_{i1}^I(t) \vee x_{i2}^I(t)...\vee x_{ik}^I(t)) & (2) \\ (x_{i1}^A(t) \vee x_{i2}^A(t)...\vee x_{ij}^A(t)) & (3) \\ \neg(x_{i1}^I(t) \vee x_{i2}^I(t)...\vee x_{ik}^I(t)) & (4) \end{cases}$$

where the ◊, ∨, and ¬ symbols are ternary HIGH/LOW PASS, OR and NOT operators, $x_{ij}^A$ is the state of the $i^{th}$ node's $j^{th}$ activator, $x_{ik}^I$ is the state of the $i^{th}$ node's $k^{th}$ inhibitor. Equation (2) is used when the node possesses both activators and inhibitors, Equation (3) when the node has only activators and Equation (4) when the node has only inhibitors. The number of state variables determines the total number of system-wide states such that a model of N state variables possesses $3^N$ states. As a result the number of total system-wide states increases rapidly as new state variable elements are added.

These calculations were encoded into a rapid-prototyping Python script that was used to search the above-mentioned network for stable equilibrium states.  Analysis time scaled approximately with N state variables as $O(N^2)$. Results of these simulations can be summarized as follows:

- In a first validation of the methodology, a discrete-network equivalent of the differential equation model used previously [1] was tested and the same two stable states were recovered. These were a normal resting state and a hypocortisolic state.

- *Male subjects*.  Inclusion of basic immune function and sex hormone regulation by the HPG axis with HPA function (HPA-GR-Immune-HPG model) *in male subjects* resulted in the emergence of 3 stable equilibrium states. Once again the first state was that of normal health. The second equilibrium state was characterized by low levels of ACTH and elevated expression of the glucocorticoid receptors GR1 and GRD1. The third state corresponded to a *hypercortisolic condition* with high glucocorticoid receptor expression (GR1, GRD1) and adaptive immune activity (AIR), accompanied by a *suppression of the HPG axis, innate immune function (IIR)* and IL-10 concentration.

- *Female subjects*. In the specific case of positive feedback along the HPG axis and suppressive interaction with the HPA axis, the HPA-GR-Immune-HPG model for female subjects (Figure 1B) supported 6 steady states. In addition to 3 states equivalent to those obtained for the male subjects, we found new steady states that corresponded to *low CRH, ACTH, and CORT*, with nominal immune function accompanied by elevated GnRH, LH/FSH, and EST. This combination occurred at each of the three low, nominal and high values for GRD1/GR1 expression. Note that a stable steady state characterized by low cortisol levels was found *only for female subjects*.

- *Alignment with experimental data*. To validate these results the predicted steady states were first compared to steroid and cytokine levels recorded in male Gulf War veterans with GWI and healthy veterans (HCs) as part of a sister study [7] (Figure 2A). To compare against model predictions steroid and cytokine levels significantly higher in GWI were assigned a value of +1, significantly lower levels were assigned -1, and those showing no significant change were assigned 0.  Experimental cytokine measurements were scored and aggregated into cytokine sets. Together with hormone levels, these data supported experimental estmates for 5 of the 11 state variables modeled. Comparison of these state variables with the predicted steady state (SS2) described by low TEST, high CORT, high AIR values, showed a match in 3 out of 5 variables for the GWI condition (Figure 2A).  As experimental measures for ACTH, GR1 and GRD1 were not available, steady state SS1 and the nominal steady state SS0 (HC) could not be distinguished and validated separately from one another.

  As a much greater proportion of women than men are affected by CFS, we compared the predicted steady states identified with the female model to experimental data collected under two compatible studies [8,9]. Taken together, experimental measurements indicated that female CFS patients presented with high EST, hypocortisolism, and with a spectrum of altered cytokine levels. We found no agreement with the low EST, high CORT and high AIR steady of steady state SS2, which closely resembled the GWI profile.  However, there was a *complete alignment* in all 5 state variables between measured levels of endocrine-immune markers in female CFS subjects and the 3 steady states characterized by high EST, low CORT and nominal immune function (SS3, SS4 and SS5 in manuscript; Appendix A).

*3.    A detailed model of immune circuitry (**Task 2, Task 5**)*. Based on the work of Folcik et al. (2007, 2011) [10,11] and an extensive review of recent literature, we constructed a wiring diagram that describes cytokine signaling between immune cell populations using the above-mentioned methodology (Figure 3) [12] (see excerpts of manuscript in preparation; Appendix B). The specific cytokines supporting this model included interleukin (IL)-1, IL-2, IL-4, IL-5, IL-6, IL-8, IL-10, IL-12, IL-13, IL-23, IL-27, interferon (IFN)-γ, and tumor necrosis factor (TNF)-α. In accordance with Folcik et al. (2011) and to improve computational efficiency, cytokines were grouped according to their dominant action into either a monokine (MK) or cytokine (CK) group. The MK groups represented the cytokines released primarily by monocytes (ie: DCs or dendritic cells) and the CK groups represented the cytokines released by lymphocytes (ie NK cells, Th cells, and CTLs). MK1 and CK1 were designed as pro-inflammatory cytokine groups, whereas MK2 and CK2 were specified as anti-inflammatory cytokine groups. See Table 4 in appendix B for the cytokine groups definitions used. It should be noted that the MK2 node in the final model also represents the anti-inflammatory dendritic cells (DC2). Since the DC2 node had only one input (Infection) and only one output (MK2), these 2 nodes were lumped into a single node consisting of the MK2 cytokines.

In order to capture interaction with the endocrine system and allow integration into the HPA-HPG-immune model described in Section 1, this detailed immune model also included the hormone inputs of cortisol and testosterone. Cortisol typically acts to suppress NK cell activity, Th1 activity and inflammatory dendritic cell

(DC) activity. Conversely it has been demonstrated that the pro-inflammatory cytokines, predominantly IL-1, IL6, and TNF-α, generally activate the HPA axis at the hypothalamic level by inducing CRH secretion leading to increased release of ACTH and eventually cortisol. With regard to the male HPG axis, studies have shown that testosterone and other androgens exert a suppressive effect on the IL-6 gene. Testosterone is also reported to enhance the Th1 response and activate cytotoxic T lymphocytes (CTLs). Cytokines can also exert negative feedback on the male HPG axis. It has been shown that receptors for the pro-inflammatory cytokines, IFN-γ and TNF-α, exist on male leydig cells and act to decrease the production of testosterone. As well, TNF-α typically down-regulates the release of GnRH in the hypothalamus and LH in the pituitary gland, eventually causing a decrease in testosterone levels. As described in the model in Section 1, testosterone, via its androgen receptor, will inhibit activity of the HPA axis while cortisol will suppress the HPG axis, inhibit the effects of testosterone, and down-regulate androgen receptor expression.

These interactions along with an updated version of the cytokine signaling network proposed by co-investigator Folcik-Nivar have been integrated into an extended model of immune signaling complete with the effects of stress and sex hormones for male subjects only at this time (Figure 3). A model for female immune-endocrine signaling, similar in level of detail, is being constructed.  As before, a first version of this model for the male system was analyzed producing results that can be summarized as follows:

- *Stable immune response modes in male subjects*. Application of this discrete dynamical analysis to the detailed endocrine-immune network yielded three different stable attractors. In addition to the normal healthy homeostatic point a first alternate attractor (SS1) was characterized by lower than normal levels of MK1, MK23, MK27, Th1 and DC1 activation, accompanied by higher than normal MK2, CK2, and Th2 activation with all other markers at nominal levels. This attractor represents an upregulated anti-inflammatory response since the anti-inflammatory cytokines (MK2 and CK2) and immune cells (Th2) are high, while all other markers remain either low or nominal. The second alternate attractor (SS2) was characterized by low relative levels of NK and Th1 activity, low testosterone combined with elevated CK1, CTLs, and cortisol with all other markers at nominal levels. This attractor represents a hypercortisolic and hypoandrogenic inflammatory state.

- *Alignment with experimental data*.  Once again, these predicted steady states were compared with experimental data used in Section 1 [7-9]. The added detail made available by this model allowed for comparison of 8 markers instead of 5. We found in GWI that expression in 7 of the 8 clinical marker sets were in alignment with the hypercortisolic/ hypoandrogenic inflammatory attractor (SS2) while none of these supported alignment with the anti-inflammatory attractor (SS1) (Figure 4A). Comparing clinical CFS data to the predicted stable attractors, we found expression in 5 out of 8 clinical marker sets were aligned with the anti-inflammatory attractor (SS1), and 6 out of 8 clinical marker sets were in alignment with the hypercortisolic/hypoandrogenic inflammatory attractor (SS2) (Figure 4B). These alignments are best visualized with a Sammon projection of the hamming distances between the clinical data and the predicted model stable states (Figure 5).

Collectively these simulations of known endocrine-immune circuitry support the existence alternate homeostatic regimes, some of which overlap substantially with observed immune and endocrine status in male GWI and female CFS subjects. Such overlap with naturally occurring stable regulatory regimes would certainly be consistent with the long-term persistence of symptoms and the chronic nature of these illnesses. This same characteristic may also explain why these illnesses appear in many ways resistant to treatment.

*4.     Early treatment surveys (**Task 6, Task 7**)*.  Analysis of the above-mentioned regulatory signaling circuits not only provides information describing the stable steady states available to the system but also extensively describes the ensemble of transitory states that lead *unequivocally* to one steady state or another; these are said to lie within that steady state's *basin of attraction*. Importantly, these subsets of transitory states will lead to that specific stable state independently of an individual's immune and endocrine response kinetics. This guaranteed convergence to a healthy equilibrium makes them attractive as broadly applicable treatment destination states. *In the design of minimally invasive interventions our basic paradigm*

*is therefore to identify the closest transitory state(s) that lie within the basin of attraction that ensures a return to normal homeostasis.*

Based on this paradigm we have started work on Tasks 6 and 7. A first preliminary analysis of the multi-system model described in Craddock et al., 2012 (Appendix A) suggests that the effectiveness of a single-agent interventions targeting the immune _or_ endocrine systems separately would be highly dependent on person-to-person differences in response kinetics. A joint endocrine-immune therapy that would moderate free cortisol and Th1 immune activity concurrently appears much more promising if we are to deliver a broadly applicable treatment protocol. We are currently refining these models as well as the treatment search algorithm to incorporate the effects of timescale. This will make it possible to take advantage of saddle point states or unstable intermediate states that lie between the basins of attraction. We are currently investigating avenues for exploiting broad classes of kinetic scales that might make it possible to reduce the treatment complexity even further and tailor these interventions to patient sub-groups.

*5.*      *Continuing work*.   Work is ongoing on the refinement of the treatment design algorithm and a working document describing initial results is being assembled as a draft manuscript. Central to this is the implementation of changes allowing for us to extend beyond connectivity and exploit differences in time scale. A second major area of ongoing work involves the design of a circuit model describing mechanisms of neuroinflammation and neurotransmission in the brain. Each component model is being designed to connect seamlessly with the other modules.

_Timeline_.  As described in the previous report dated September 30, 2011, the University of Alberta's Research services Office submitted on behalf of the principal investigator a request for a one-year extension of the project term due to administrative delays. This request was reviewed initially by Ms. Strock and Dr. Phillips of the DoD (January 23, 2012) and we were asked to resubmit this request at a later date (6-8 months before end of project term). We have since confirmed with Dr. Rebecca Fisher that this continues to be the correct course of action (ref. email from Dr. Fisher dated September 21, 2012). In accordance with Dr. Fisher's recommendation we plan to submit a formal request for a no-cost extension in May 2013.

**Key Research Accomplishments**.
In keeping with the milestones described in the project submission initial efforts were directed at:

- We have completed Task 1. Based on work reported previously we revised the modeling approach and adopted a logic circuit paradigm that allows us to draw on a much larger body of anatomical and biochemical knowledge while also providing the flexibility to seamlessly incorporate kinetic data when available. This approach was originally deployed in a high-level Python code but has recently been re-engineered into a highly efficient C code. This has resulted in an order of magnitude improvement in execution speed and memory usage.

- We have essentially revised and completed Task 2. We completed a careful audit of the original Basic Immune Simulator (BIS) model and a thorough review of the most recent literature related to the relevant immune signaling mechanisms. Based on this we updated and translated the BIS into a logic circuit model and have analyzed the dynamic stability properties of this regulatory network.

- We have made substantial progress in the central component Task 3. In this regard we have produced and analyzed a circuit model combining a formal representation of interactions within and between the HPA axis, the HPG sex hormone axis and basic components of the immune system.

- Consistent with Task 4 we have conducted an analysis of multi-stability properties of both the broad HPA-HPG-immune model and the detailed BIS immune model. Based on this analysis we then compared the predicted equilibrium states obtained from each model with experimental immune and endocrine data from male and female GWI and CFS subjects. We found substantial alignment of GWI with stable steady states involving a hypercortisolic/ hypoandrogenic status.

- One complete manuscript is currently undergoing final internal review and another is in the final stages of completion with submission expected before year's end.

- We have re-assessed our approach to treatment design (<u>Task 6, 7</u>) and have begun a preliminary search based on the HPA-HPG-immune model described above. Initial results support a combined hormone-immune therapy.

**<u>Reportable Outcomes</u>**.
The results of these latest analyses are being presented at an upcoming closed meeting sponsored by the CDC and the CFIDS Association of America and held at the Cold Spring Harbor Laboratory's Banbury Centre in Long Island, NY (Sep. 30 -Oct 3, 2012). The draft manuscript Craddock et al., 2012, enclosed as Appendix A, is completing internal review by co-authors and we expect submission to the journal PLoS Computational Biology before Oct. 1, 2012. Similarly we expect the working document in Appendix B, Fritsch et al., 2012, to be ready for submission to the same journal by year's end.

Regarding synergy with complementary research efforts, these findings were recently used in the preparation of an invited GWIRP Consortium Award as planned under Consortium Development Award GW100070 (prime institution - Wright State University).

**<u>Conclusions.</u>**
We intend to file in May 2013 a formal request for a no-cost extension of the project term due to a delayed start. We have carried out a major shift in paradigm that ensures greater flexibility and will support the necessary breadth of the project. The basic algorithmic framework for this is now in place. Both the BIS model of immune signaling and the basic model of the HPA axis have been audited, updated and extended significantly. Both models have now been translated into this new formalism. Simulations based on these models have shown that the illness-specific effects of gender are particularly striking. Work continues on the refinement of the intervention design component. Initial analyses favor the deployment of a joint hormone-immune intervention over strategies that target these systems separately.

**<u>Personnel receiving support from this award</u>**:

- Travis Carddock, Ph.D., Senior Research Associate, Broderick Laboratory, University of Alberta
- Paul Fritsch, undergraduate Honors Physiology student, Research Intern, Broderick Laboratory, University of Alberta

**<u>References</u>**.
1.    Ben-Zvi A, Vernon SD, Broderick G. 2008. Model-based Therapeutic Correction of Hypothalamic Pituitary Adrenal Axis Dysfunction. PLoS Comput Biol 5(1): e1000273. doi:10.1371/journal.pcbi.1000273.

2.    Crofford LJ, Young EA, Engleberg NC, Korszun A, Brucksch CB, McClure LA et al. Basal circadian and pulsatile ACTH and cortisol secretion in patients with fibromyalgia and/or chronic fatigue syndrome. Brain Behav Immun 2004; 18:314-25.

3.    Thomas R, Thieffry D, Kaufman M (1995) Dynamical behaviour of biological regulatory networks--I. Biological role of feedback loops and practical use of the concept of the loop-characteristic state. Bull Math Biol. 57: 247-276.

4.    Thomas R (1991) Regulatory Networks Seen as Asynchronous Automata: A Logical Description. J Theor Biol 153: 1-23.

5.    Mendoza L, Xenarios I (2006) A method for the generation of standardized qualitative dynamical systems of regulatory networks Theor Biol Med Model 3: 13

6.    Craddock TJA, Miller DB, Fletcher MA, Klimas NG, Broderick G. Towards an Integrative Model of Complex Stress-Mediated Illnesses: Gulf War Illness and Chronic Fatigue Syndrome. 2012, Under internal review for submission to *PLoS Comput Biol*.

7.    Broderick G, Kreitz A, Fuite J, Fletcher MA, Vernon SD, Klimas N. A pilot study of immune network remodeling under challenge in Gulf War Illness. Brain Behav Immun. 2011 Feb; 25(2): 302-13.

8.  Broderick G, Fuite J, Kreitz A, Vernon SD, Klimas N, Fletcher MA. Formal Analysis of Cytokine Networks in Chronic Fatigue Syndrome. Brain Behav Immun, 2010 Oct; 24(7): 1209-17.

9.  Fuite J,Vernon SD, Broderick G. Neuroendocrine and Immune Network Re-modeling in Chronic Fatigue Syndrome: An Exploratory Analysis. Invited submission, Genomics 2008; 92(6): 393-399.

10. Folcik VA, An GC, Orosz CG.cThe Basic Immune Simulator: an agent-based model to study the interactions between innate and adaptive immunity. Theor Biol Med Model. 2007 Sep 27;4:39.

11. Folcik VA, Broderick G, Mohan S, Block B, Ekbote C, Doolittle J, Khoury M, Davis L, Marsh CB. Using an agent-based model to analyze the dynamic communication network of the immune response. Theor Biol Med Model. 2011 Jan 19;8:1.

12. Fritsch P, Craddock TJA, Smylie AL, Folcik Nivar VA, Fletcher MA, Klimas NG, de Vries G, Broderick G. A Study of Multiple Homeostatic Regimes in a Discrete Logic Model of Immune Signaling. 2012. In preparation.
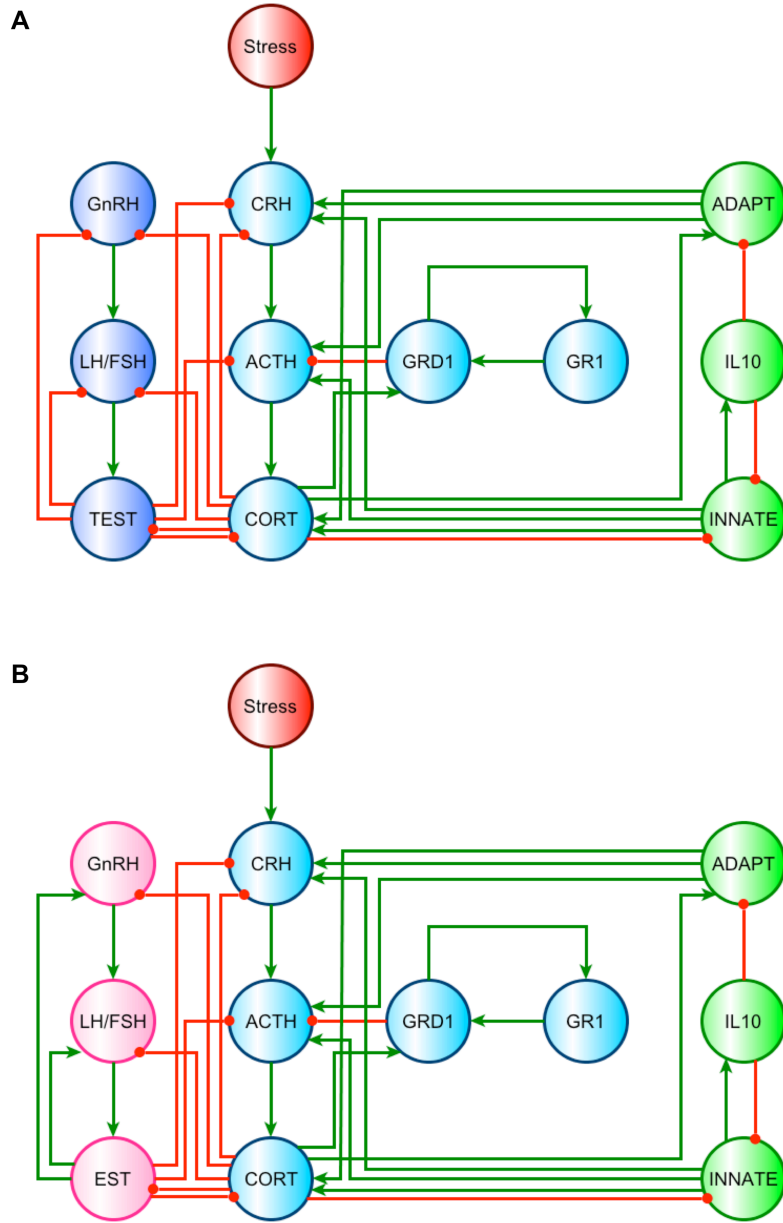
**Figure 1**. A discrete circuit model of HPA-HPG-immune interactions in male subjects (A) and female subjects (B) in the specific case of positive feedback along the female HPG axis and suppressive interaction with the HPA axis (model c in the manuscript) [6]. Green directed edges represent an up-regulation of the target by the source node whereas a red terminal edge represents a suppressive action.
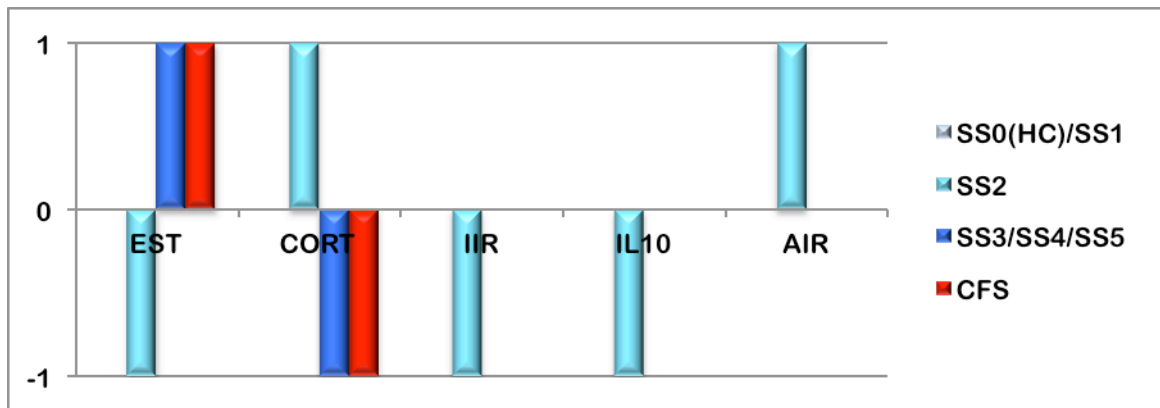
**A.**
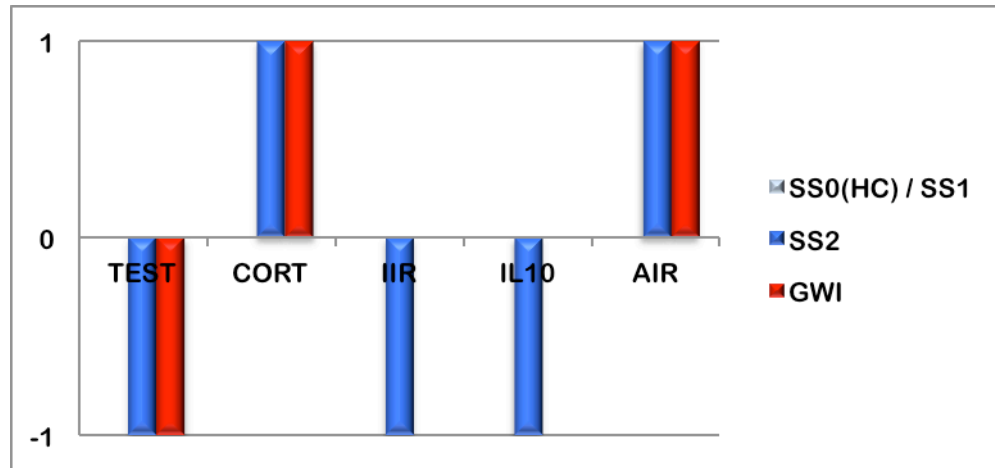


**B.**



**Figure 2**. Alignment between the stable states (SS0, SS1, SS2) predicted by the circuit model and the discrete expression  (e.g. elevated (+1), normal (0), or suppressed (-1)) of 5 markers in experimental data from (A) male GWI subjects and (B) female CFS subjects [6].
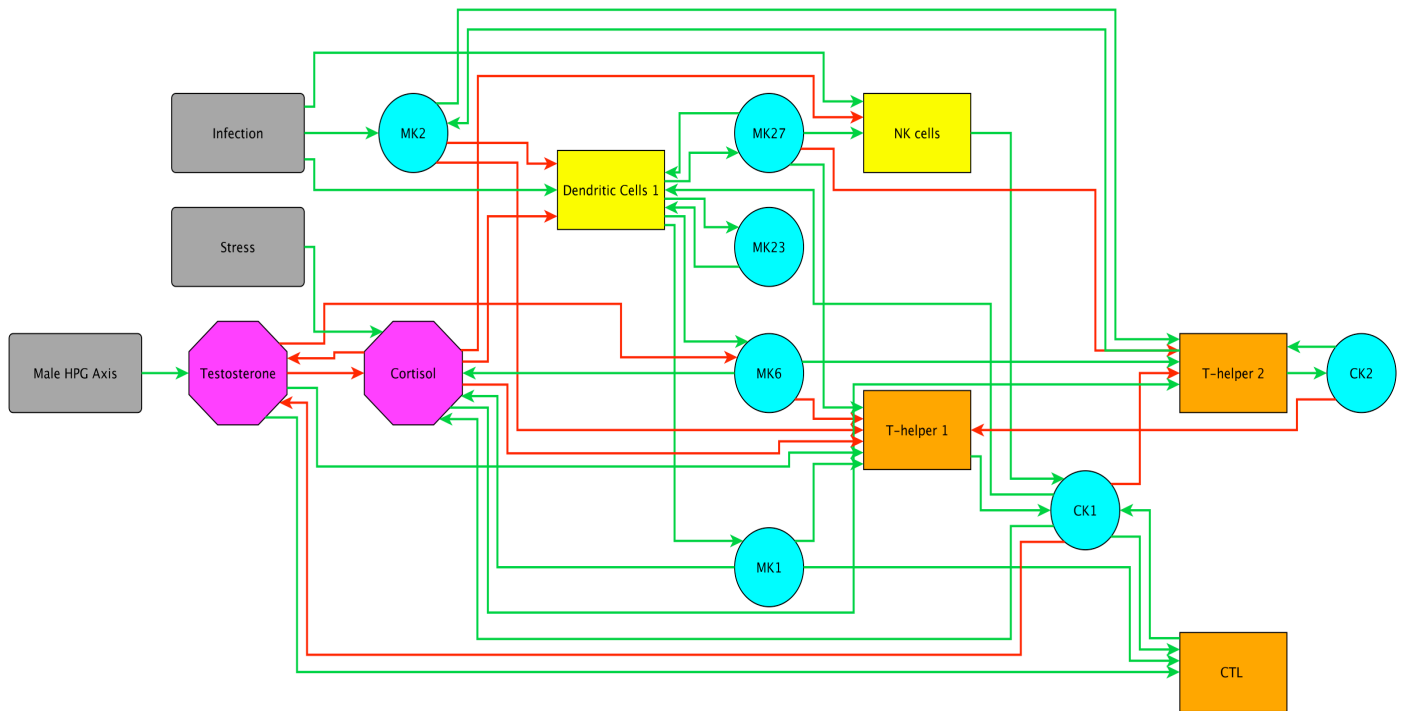
**Figure 3**. Wiring diagram for a circuit model of the immune signaling network with hormonal inputs from cortisol and testosterone (purple). The nodes, Stress, Infection, and Male HPG axis (grey) were necessary components of the program required as inputs, but they were kept consistently nominal so they would have no effect on the overall network as per the logical functions. Green connections indicate an activating influence and red connections indicate an inhibiting influence [12].
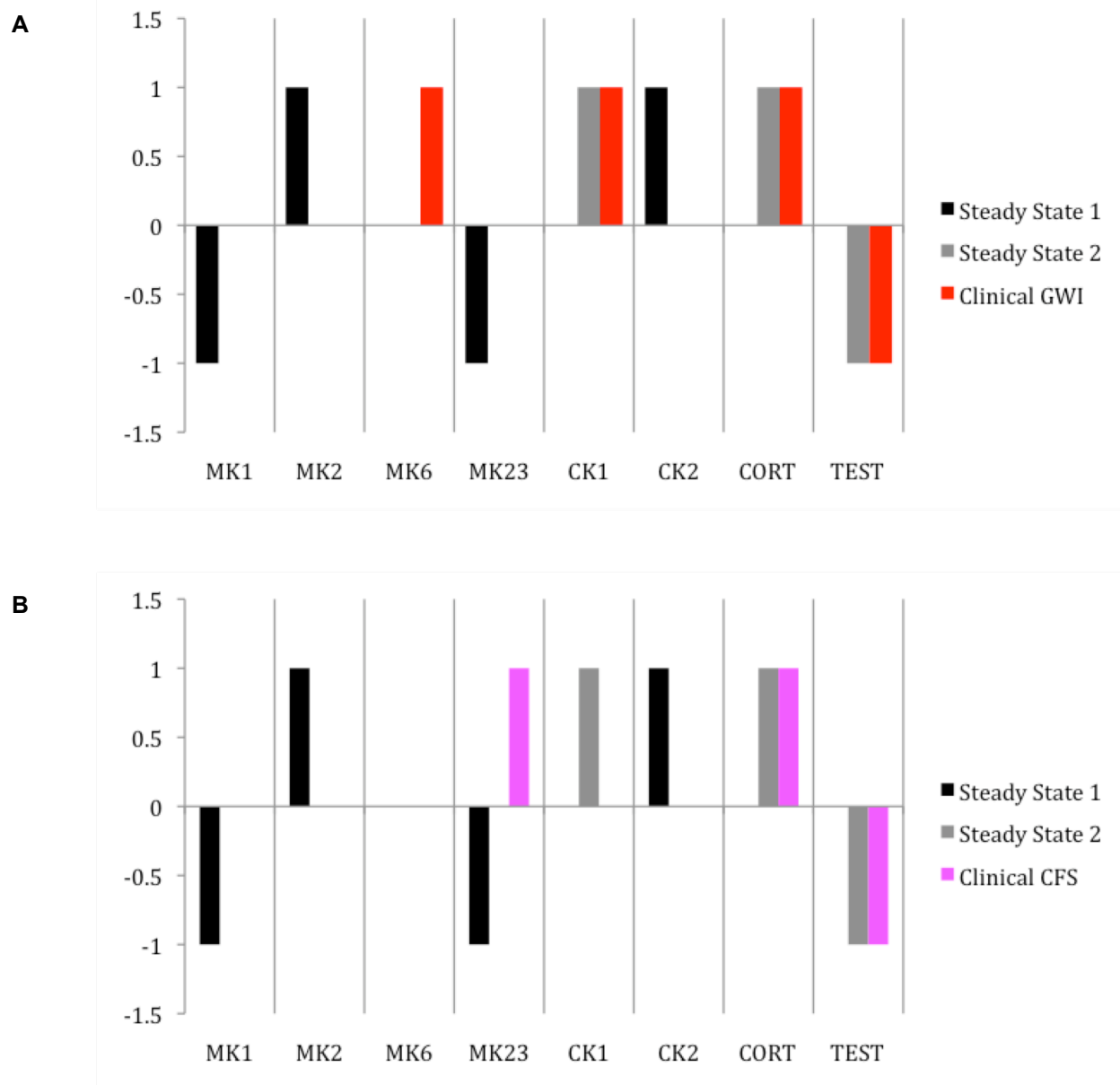
**Figure 4**. Discretized experimental data for (A) GWI and (B) CFS compared to the two predicted alternate stable steady states (SS1 [black] and SS2 [grey]) [12].
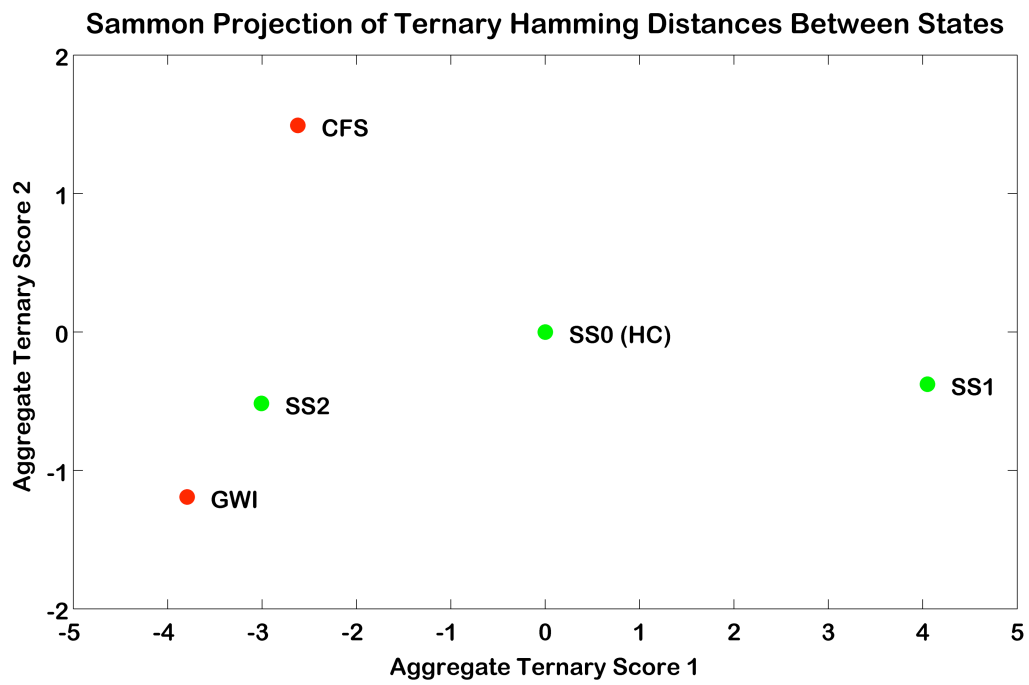
**Figure 5**. Sammon projection of the hamming distances between all five stable system states. Green circles represent the predicted model attractor states (SS0(HC), SS1, and SS2). Red circles represent the aggregated clinical data for GWI and CFS [12].

**Appendix A**:

Craddock TJA, Miller DB, Fletcher MA, Klimas NG, Broderick G. Towards an Integrative Model of Complex Stress-Mediated Illnesses: Gulf War Illness and Chronic Fatigue Syndrome. 2012, *Under internal review*.

# Towards an Integrative Model of Complex Stress-Mediated Illnesses: Gulf War Illness and Chronic Fatigue Syndrome

Travis J. A. Craddock **[1], Paul Fritsch[1], Diane B. Miller[2], Mary Ann Fletcher[3], Nancy G. Klimas[4], and Gordon Broderick ** [1,3]


[1]Department of Medicine, Faculty of Dentistry and Medicine, University of Alberta, Edmonton, Alberta, Canada

Ph: +1-780-552-3894          Email: travisc@ualberta.ca

Ph: +1-780- 232-9312          Email: pfritsch@ualberta.ca

Ph: +1-780-492-1633          Email: gordon.broderick@ualberta.ca

[2]Centers for Disease Control and Prevention, National Institute for Occupational Safety and Health, Morgantown, West Virginia, USA

Ph: +1-304-285-5732          Email: dum6@cdc.gov

[3]Department of Medicine, Miller School of Medicine, University of Miami, Miami, Florida, USA

Ph: +1- 305-243-6525          Email: MFletche@med.miami.edu

[4]Department of Medicine, Nova Southeastern University, Fort Lauderdale, Florida, USA

Ph: +1- 305-575-3267          Email: nklimas@nova.edu


** Corresponding author

Dr. Travis Craddock, Research Associate/ Dr. Gordon Broderick, Associate Professor

Dept. of Medicine, University of Alberta, WMC 2E4.41 WC Mackenzie Health Sciences Ctr.

8440 - 112 Street, Edmonton AB T6G 2R7, Canada

Ph: +1-780-552-3894; 492-1633  Email: travisc@ualberta.ca;  gordon.broderick@ualbert.ca

**Abstract**

As a key component in the body's stress response system, the hypothalamic-pituitary-adrenal (HPA) axis serves to orchestrate changes across a broad range of major biological systems, and its dysfunction has been associated with numerous chronic diseases including Gulf War Illness (GWI) and chronic fatigue syndrome (CFS). Though tightly coupled with other components of endocrine and immune function, few models of HPA function account for these interactions. An important obstacle has been the scarcity of *in vivo* kinetic data.  Here we extend conventional models of HPA function by including feed-forward and feedback interaction with sex hormone regulation and immune response. This is accomplished using a discrete logic representation based solely on documented physiological and biochemical connectivity without detailed response kinetics.  A circuit model linked state variables across the HPA axis, hypothalamic-pituitary-gonadal (HPG) function, both in men and women, as well as innate (IIR) and adaptive (AIR) immune response described in terms of specific cytokine sets. Results indicated that unlike current models, detailed representation of glucocorticoid receptor dimerization is not required to produce multi-stability when immune and sex hormone regulation are considered. Inclusion of these effects resulted in at least two alternate homeostatic regimes. Experimental data in male GWI subjects showed alignment in 3 of 5 endocrine-immune markers with predictions of a naturally occurring steady state. In female CFS subjects, the expression of all 5 endocrine-immune markers aligned with an alternate homeostatic state predicted by the model based on regulatory circuitry. Indeed we found that hypercortisolism may be inextricably linked to an imbalance in the immune response whereas hypocortisolism may be more strongly related to sex steroid suppression of the HPA axis and promotion of HPG function, a configuration seemingly available only to female subjects. Though coarse, these models may nonetheless support the design of simple and robust treatment avenues.

**Author Summary**

The hypothalamic-pituitary-adrenal (HPA) axis links the brain, endocrine and immune systems of the body, and serves as a major regulator of the body's response to stress including emotion, digestion, metabolism, sensory perception, etc.… Not surprisingly, dysregulation of the HPA axis has been associated with numerous chronic diseases, of which Gulf War Illness (GWI) and chronic fatigue syndrome (CFS) are two examples. While HPA function is inextricably linked with that of its regulatory neighbors few models account for these all-important interactions, as many of the key parameters needed have yet to be determined experimentally. Here we extend the common models of the HPA axis by including interaction with sex hormone regulation and immune response. We use documented physiological and biochemical data to construct a connectivity network describing these systems for both men and women, and apply a discrete logic to represent the states of the system qualitatively without the need for kinetic parameters. Results indicate that this extended system can accommodate other naturally occurring persistent states in addition to healthy response to stress. Two of these alternate resting states align with experimental data describing GWI and CFS subjects.

## 1. Introduction

The hypothalamic-pituitary-adrenal (HPA) axis, a key component in the body's stress response system, serves to articulate changes in broad range of homeostatic regulators as a function of environmental cues. Such cues can consist of both physical stressors (injury, disease, thermal exposure) and psycho-emotional stressors (frustration, fear, fight or flight decisions) alike. Instantiation of this survival program is accomplished through controlled modulation of the neuroendocrine and immune systems, as well as the sympathetic nervous systems [1-3]. Considering its function as a broad-reaching integrator of major biological systems, it is no surprise that numerous chronic diseases have been associated with abnormal regulation of the HPA axis, including major depression [4, 5], post-traumatic stress disorder (PTSD) [6-8], Alzheimer's disease [9], Gulf War illness (GWI) [10-12], and chronic fatigue syndrome (CFS) [13-15]. When compared to non-deployed veterans, Golier et al., (2007) [10] found that symptomatic Gulf War veterans without psychiatric illness, as well as veterans with PTSD alone, showed significantly greater cortisol suppression to dexamethasone (DEX) suggesting markedly enhanced negative feedback along the HPA axis. Further study by these same investigators indicated that this might be due to a significantly attenuated ACTH response by the pituitary in veterans with GWI without PTSD compared to non-exposed subjects and veterans with PTSD alone [11, 12]. A similar suppression of cortisol response to DEX was found in CFS subjects by Van Den Eede et al. (2007) [13] with this being further exacerbated by oestrogen intake. With regard to HPA circadian dynamics, CFS subjects were found to exhibit significantly increased ACTH-adrenal signaling and marginally increased inhibitory feedback when compared with control subjects and CFS subjects comorbid with fibromyalgia (FM) [14, 15]. Conversely the pain-dominant CFS-FM subjects showed significantly blunted cortisol inhibitory feedback. While evidence such as this implicates abnormal regulation of HPA function leading to chronic hypocortisolic and hypercortisolic states in these illnesses, it is not clear what causes this dysregulation.

Previously we investigated the possibility that some of these pathological states may coincide with naturally occurring states of the regulatory system in question [16]. These backup regimes would offer alternate homeostatic control in crisis situations but at the cost of reduced function. The existence of such multiple stable states is characteristic of systems that incorporate feed-forward and feedback mechanisms.

20

Feedforward loops in biology play the crucial role of driving rapid acute responses, while feedback loops will generally limit the extent of a response. Both will also drive complex dynamic behavior, including differentiation and periodicity [17]. Under standard conditions such systems tend to reside in a given stable attractor state. Small perturbations to the system force it to depart temporarily from this state, only to be drawn back to the original resting state once the perturbation is removed. If however, the perturbation is of significant strength and duration, the system may abandon its normal operating regime and instead be drawn into the basin of attraction of a new alternate resting state. Knowledge of the system dynamics can allow us to map these different regimes and several mathematical models of the HPA exist [18-26]. However only one such model so far is known to accommodate multi-stability in the dynamic behavior of the HPA axis. It does so via the addition of a feed-forward mechanism involving dimerization of the glucocorticoid receptor (GR) complex [27] (Figure 1). However, this model and the majority of other models do not extend beyond the physiological boundaries of the HPA axis itself. As discussed in the following sections, HPA activity is intertwined with the behavior of the hypothalamic-pituitary-gonadal (HPG) axis and the immune system, among others, and this interplay cannot be ignored when considering the number and nature of stationary states available to the overarching system.

There is a substantial body of anatomical and biochemical data for many biological systems describing the connectivity between elements, the presence of recurring structural motifs and functional modules. However data regarding the precise stoichiometry and kinetics of these systems in humans is extremely limited. Many existing models rely heavily on animal data as a source of kinetic parameters, or adopt general order of magnitude estimates when this data is lacking. To circumvent this issue and draw on this rich body of physiological and biochemical wiring diagrams, we have adopted the discrete logical network methodology proposed originally by Thomas et al. [28, 29] and developed further by Mendoza and Xenarios [30]. The latter makes it possible to identify the number of resting states, their type as well as their molecular and cellular description without detailed knowledge of their response dynamics. In this work we use this method to extend our previous analysis of the complex dynamical behavior of the human HPA axis by including its regulatory interactions with the neighboring HPG axis and the immune system. Based on connectivity information alone, we show that multi-stability is easily obtained from these interacting systems.

21

Moreover, alternate resting states are identified that align with experimental data from our on-going studies of GWI and CFS.

## 2 Methods

### 2.1 A Multi-systems Model

There is a substantial amount of physiological data describing the HPA, HPG and immune systems as stand-alone entities. To a much lesser degree there also exists evidence for the mutual interactions between these systems. The following sections describe the experimental evidence used to infer the topology of an overarching HPA-HPG-immune interaction network (Figures 1-4).

### 2.1.1 The HPA Axis

Activation of the HPA axis begins at the paraventricular nucleus (PVN) of the hypothalamus. Specifically, afferents transmitting stress related information in the brain converge on the medial parvocellular neurons of the PVN inducing the release of several peptides, including corticotropin-releasing hormone (CRH) and arginine vasopression (AVP), into the pituitary hypophysial-portal circulation. CRH and AVP act in conjunction on membrane bound CRH-R1 receptors in the anterior pituitary to stimulate adrenocorticotropic hormone (ACTH) synthesis, and its rapid release into peripheral circulation. ACTH circulates to the adrenal cortex where it acts on the membrane bound MC2-R receptor to simulate the release of glucocorticoids (GCs) (corticosterone in the rat and cortisol (CORT) in humans and nonhuman primates). To regulate the stress response, GCs exert negative feedback at the hypothalamus and pituitary to inhibit further synthesis and release of CRH and ACTH, respectively [31]. This is the standard view of the HPA axis utilized in the majority of models (Figure 1 A). However, as noted by Gupta et al. [27] circulating glucocorticoids act via cytostolic GC receptors (GRs), which, unlike membrane bound receptors, dimerize (GRD) and translocate into the cell nucleus upon activation to up-regulate GR synthesis and interact with other relevant transcription factors, or GC-sensitive genes (Figure 1 B). As all nucleated cells possess GRs, GCs influence practically every system in the body. As described below major systems affected by GCs include the HPG axis and immune system.

## 2.1.2 The HPG Axis

GCs have an inhibitory effect on the HPG axis, a key component that controls development and regulation of the reproductive system, at all levels [32-36]. Activation of the HPG starts from brain generated pulsatile signals that stimulate the preoptic area of the hypothalamus to produce gonadotropin-releasing hormone (GnRH).  GnRH is secreted into the pituitary hypophysial portal bloodstream, which carries it to the pituitary gland, where it activates membrane bound GnRH-R receptors, resulting in the synthesis and secretion of luteinizing homone (LH) and follicle-stimulating hormone (FSH) into circulation.  These gonadotropins flow to the gonads where they work synergistically to promote the secretion of the sex steroids.  In males, LH binds to receptors on Leydig cells in the testes to stimulate the synthesis and secretion of testosterone (TEST).  In females, LH activates receptors on Theca cells in the ovaries to stimulate the release of androstenedione, which is aromatized by granulosa cells to produce estradiol (EST), and progesterone (PROG).  TEST negatively feeds back on the HPG to inhibit GnRH, FSH and LH secretion and synthesis [27].  This feedback mechanism is somewhat more complex in females where, depending on the phase of the female menstrual cycle, EST and PROG can exert either positive or negative feedback on the production and release of GnRH and the gonadotropins  [35, 37].

A lesser-known aspect is that several components of the HPG axis exert reciprocal effects on the HPA axis [32, 33, 35]. Thus, an interactive functional cross talk exists between the HPA and HPG axes, which cannot be ignored when investigating HPA axis regulation and dysfunction.  Testosterone exhibits an inhibitory effect on all levels of the HPA [27] (Figure 2 A), whereas EST and PROG can serve to stimulate or inhibit the HPA axis depending on menstrual cycle phase, or phase of life [33].  It is not clear whether the EST and PROG inhibition/stimulation of the HPA occurs in coordination with the inhibition/stimulation of the HPG.  As a result, these cases were explored as separate alternative models of the HPA-HPG interaction (Figure 2 B-D).

## 2.1.3 A Simplified Model of the Immune System

While not typically considered part of the neuroendocrine system, the immune system plays a very important role in regulating the HPA axis.  As with the HPG axis, there exists a mutual crosstalk between

these two systems [38-40]. The innate immune response (IIR) is regulated by cytokines produced primarily by mononuclear phagocytes, such as macrophages, and dendritic cells, however they may also be produced by T-lymphocytes, natural-killer (NK) cells, endothelial cells or mucosal epithelial cells. These cytokines include the pro-inflammatory cytokines interleukin (IL) -1, IL-6, IL-8 and tumor necrosis factor alpha (TNF-$\alpha$), and can also include IL-12, a primary mediator of early IIR. Also included is IL-15, which stimulates proliferation of NK cells and effector T-lymphocytes, as well as IL-23, an important inflammatory signal contributing to the Th17 response against infection. Cytokines that regulate the adaptive immune response (AIR) come primarily from T-lymphocytes that have recognized a cell-specific antigen. These include IL-2, IL-4, IL-5, IL-13, interferon-gamma (IFN-$\gamma$), and TNF-$\beta$. IL-10, which has important anti-inflammatory and immunosuppressive activities, is primarily produced by macrophages, but is also produced by T-lymphocytes, dendritic cells, neutrophils, eosinophils, mast cells, B cells, NK cells, CD8$^+$ T cells, and all CD4$^+$ T-helper cells, and is therefore considered separate from both the IIR and AIR [41].

The cytokines of the IIR and AIR all serve to stimulate the HPA axis at all levels [38-40]. GCs, in turn, serve to suppress the synthesis and release of the pro-inflammatory cytokines of the IIR, while causing a shift from the inflammatory response to the anti-inflammatory response and promotion of the AIR [38, 39, 42]. In the simplified model used here, the effect of the key regulating cytokine IL-10 is produced primarily by IIR with suppressive effects on both IIR and AIR (Figure 3).

### 2.1.4 An Integrative Model of the HPA-HPG-Immune System

The interactions of the HPA, HPG and immune systems outlined above provide the basis for a simplified model that nonetheless encompasses a broad set of the major interactions that link these systems. Analyzing the components of this model in a piecewise fashion can highlight the involvement of each individual system in the resulting stable attractor states. Piecewise combination of the above HPG and immune systems with the HPA involves 10 individual steps (Figures 1-4 and S6). However, as the action of CORT is accompanied by up-regulation of GR synthesis all connections involving CORT can include the GR-GRD feed-forward mechanism. As such, the GR-GRD feedback loop was also added piecewise to major components of the HPG and immune systems over 29 different steps (Figures 1-4 and S1-S9). At

each step the resulting HPA axis and extended system was analyzed via a discrete state representation to solve for the stable states.


## 2.2 A Discrete State Representation

Following the methods of Thomas et al. [28, 29], and more recently Mendoza and Xenarios [30], connectivity network models of the neuroendocrine-immune system are represented as a discrete series of interconnected elements with three states: -1 (inhibited), 0 (nominal) and 1 (activated). The current state of all nodes in the system is described by a state vector $\vec{x}(t)$, such that:

$$\vec{x}(t) = (x_1(t), x_2(t)...x_N(t)) \tag{1}$$

where $x_N(t)$ is the state of the $N^{th}$ node of the system at time $t$. The preferred state towards which the system evolves in the next time increment is described by the image vector $\vec{x}(t+1)$. The state value of the image vector for the $i^{th}$ node in the system is determined from the node's current state and a set of balanced ternary logic statements based on the state values of the neighboring input nodes and their mode of action (i.e. activate or inhibit). The logic statements that determine a state transition are expressed as follows (Eq. 2-4):

$$x_i(t+1) = \begin{cases} (x_{i1}^A(t) \lor x_{i2}^A(t)... \lor x_{ij}^A(t)) \lozenge (x_{i1}^I(t) \lor x_{i2}^I(t)... \lor x_{ik}^I(t)) & (2) \\ (x_{i1}^A(t) \lor x_{i2}^A(t)... \lor x_{ij}^A(t)) & (3) \\ \neg (x_{i1}^I(t) \lor x_{i2}^I(t)... \lor x_{ik}^I(t)) & (4) \end{cases}$$

where the $\lozenge$, $\lor$, and $\neg$ symbols are ternary HIGH/LOW PASS, OR and NOT operators, $x_{ij}^A$ is the state of the $i^{th}$ node's $j^{th}$ activator, $x_{ik}^I$ is the state of the $i^{th}$ node's $k^{th}$ inhibitor. The ternary operators given in Equations (2) through (4) are described in further detail in Supplementary Tables S1- S3. Equation (2) is used when the node possesses both activators and inhibitors, Equation (3) when the node has only activators and Equation (4) when the node has only inhibitors.

Applying Equations (2)-(4) to each node in the network for a given state of the system, $\vec{x}^m(t)$, defines the image vector $\vec{x}^m(t+1)$ for $m^{th}$ state of the system. With $\vec{x}^m(t+1)$ defined, the system may be updated asynchronously following the generalized logical analysis method of Thomas et al. [28, 29]. According to this method the $i^{th}$ element of the $m^{th}$ state vector $\vec{x}^m(t)$ is moved one step towards its preferred image $\vec{x}^m(t+1)$ (e.g. If $\vec{x}^m(t)$ = -1 and $\vec{x}^m(t+1)$ = 1, then $\vec{x}_i(t)$ is set to 0). Thus, for each current state of the system there are potentially several subsequent states towards which it may asynchronously evolve.

By analyzing all possible states of the system a temporal sequence of all logical states may be discerned. To interpret the results each state of the system can be represented as a node in a state network. The evolution from one state to a subsequent state is then represented as a directed edge between the two state nodes. Representation of the system state trajectory in this fashion makes it possible to draw on the concepts and tools of network theory for analysis of the system dynamics. Steady states are defined as those states for which the image vector is the same as the current state vector; in other words the state node possesses an out degree of 0.

Twenty-nine different piecewise steps of the HPA axis models were analyzed to solve for stable states (Table S4). The number of state variables determines the total number of system-wide states available to a model, such that a model of N state variables possesses $3^N$ states. Due to this rule the number of total system-wide states increases rapidly as new state variable elements are added. An in-house Python script was used to analyze the state network to search for states with an out degree of 0. Analysis time approximately scales with N state variables as $O(N^2)$, with minor deviations from this due to methods of parallelization, and other processes not directly related to the analysis.

### 2.3 Sample Collection, Processing and Analysis

### 2.3.1 CFS Cohort

Endocrine measurements in peripheral blood mononuclear cells (PBMC) were obtained from the Wichita Clinical dataset [43] for a group of 39 female CFS subjects and 37 Healthy controls (HCs) screened for

confounding medical or psychiatric conditions. Diagnostic classification adheres to the CFS research case definition [44]. Collection and processing of PBMCs including microarray hybridization are found in [43]. Ethics statements and details of subject screening, data preprocessing, normalization, outlier detection and false discovery correction are available in [45, 46].

Cytokine profiles were obtained from a separate study conducted at the University of Miami where CFS subjects were diagnosed using the International Case Definition [47, 48]. Those subjects presenting with additional medical and psychiatric conditions were excluded from the study, resulting in a cohort of 40 female CFS subjects and a group of 59 healthy female control subjects. Profiling of cytokine concentrations was performed in morning blood plasma samples using an enzyme-linked immuno-absorbent assay (ELISA)-based assay. Ethics statements and details of subject screening, data preprocessing, normalization, outlier detection and false discovery correction are available in Broderick et al. [49].

### 2.3.2 GWI Cohort

Cytokine profiles and endocrine measures were obtained as part of a larger ongoing study of 27 GWI and 29 HC subjects recruited from the Miami Veterans Administration Medical Center. Subjects were male and ranged in age between 30 and 55. Inclusion criteria was derived from Fukuda et al. [48], and consisted in identifying veterans deployed to the theater of operations between August 8, 1990 and July 31, 1991, with one or more symptoms present after 6 months from at least 2 of the following: fatigue; mood and cognitive complaints; and musculoskeletal complaints. Subjects were in good health prior to 1990, and had no current exclusionary diagnoses [47]. Use of the Fukuda definition in GWI is supported by Collins et al. [50]. Control subjects consisted of gulf war era sedentary veterans and were matched to GWI subjects by age, body mass index (BMI) and ethnicity. Ethics statements, methods for subject assessment, blood analysis, and data preprocessing, normalization, outlier detection and false discovery correction are available in Broderick et al. [51].

### 2.3.3 Statistical Analysis

All cohort data was normalized using a Log2 transformation. A one-tailed t-test for unequal sample sizes with unequal variance was used to determine if marker levels changed significantly between subject groups in the direction predicted by the model. Significance levels were ranked according to the null probability p with values less than 0.01 considered highly significant, values ranging from 0.01 to 0.05 considered significant, values between 0.05 and 0.10 considered marginally significant. Null probability values exceeding 0.10 were interpreted as non-significant.

The above-mentioned experimental data made it possible to compare the expression of five markers, namely TEST/EST, CORT, IIR, IL-10, and AIR, in subjects from these illness groups with predictions from the model.  All experimental data was translated from a continuous scale to a discrete scale; steroid and cytokine values found to be significantly higher in patient data were assigned a discrete value of 1, while those found to be significantly lower were valued at -1.  Those showing no significant change were assigned a value of 0.  In the case of aggregate immune state variables (i.e. IIR, IL-10, and AIR) the average of the discrete state scores for the individual cytokines falling within each set was computed and rounded to the nearest integer to provide an overall discrete score. Section 2.1.3 defines the cytokines supporting each state variable node.  Alignment between the experimental data and model estimates was computed using only exact matches.  If the experimental score and model prediction for a given state variable were opposite one another (i.e. +1 vs. -1) or if one presented an inactive state while the other scored as active (i.e. 0 vs. +1 or -1) an alignment score of zero was assigned.

**3 Results**

**3.1 Stable States in the Standard HPA Models**

Application of the discrete state representation to the stand-alone HPA model (Figure 1 A) generated 27 system states, and failed to produce multiple stable states (Table 1).  This is consistent with previous ordinary differential equation based models of the stand-alone HPA axis [16-21] [21-26], which did not show system multi-stability.  Discrete state representation of the HPA-GR model (Figure 1 B) generated 243 system states.  Of these, 2 system state nodes possess no outbound edges and are stable attractor steady states (Table 1).  In the first steady state, $\vec{x}(t) = (0,0,0,0,0)$, all state variables assume nominal values.  In

the second steady state, $\vec{x}(t) = (0, -1, -1, 1, 1)$, state variables GRD1 and GR1 are activated while ACTH and

CORT are depressed.  These states are consistent with the ordinary differential equation models of the

HPA-GR system used by Gupta et al. [27] and Ben Zvi et al.  [16].


## 3.2 The Gender Contribution

Inclusion of the HPG axis with the stand along HPA axis (Figure 2) generated 729 system states and

yielded only one steady state where all state variables assume nominal values (i.e. $\vec{x}(t) = (0,0,0,0,0,0)$ ),

except in the case of HPG model c (Table S7).  In model HPA-HPGc the inhibition of the HPA axis by the

HPG, coupled with the positive feedback loop along the HPG produced an additional steady state,

$\vec{x}(t) = (-1, -1, -1, 1, 1, 1)$, characterized by low CRH, ACTH and CORT, and high GnRH, LH/FSH and EST.


When the HPA-GR model is coupled with the basic HPG axes 6561 system states are produced.  Two

stable steady states are generated for HPG models a, b and d (Figures S1-S2, Table S7).  However, rather

than reproducing the low CORT seen in the HPA-GR model, CORT is held to its nominal value while ACTH

is low and GR1, GRD1, GnRH, LH/FSH and EST are high (i.e. $\vec{x}(t) = (0, -1, 0, 1, 1, 1, 1)$ ).  The loss of the

hypocortisolic state results from the effect of the sex steroids on CORT.  Instead of CORT receiving only a

single input it now receives multiple inputs, influencing its overall response. In the case of model c (HPA-

GR-HPGc) 5 steady states were obtained (Figures S2 and Table S7).  In addition to the two steady states

obtained with HPA-GR-HPG models a, b and d, there exist 3 new steady states characterized by low CRH,

ACTH and CORT, and high GnRH, LH/FSH and EST.  The GR1 and GRD1 values simultaneously alternate

from low to nominal to high to give the 3 new attractor states (i.e. $\vec{x}(t) = (-1, -1, -1, -1, -1, 1, 1, 1)$,

$\vec{x}(t) = (-1, -1, -1, 0, 0, 1, 1, 1)$, $\vec{x}(t) = (-1, -1, -1, 1, 1, 1, 1, 1)$ ).


Inclusion of the GR-GRD dimerization feedback loop on the HPG axis at LH/FSH, and TEST/EST (Figures

S3 and S4), produced 531441 system states and further increased the number of stable steady states.

Here the addition of the GR-GRD loop generates different profiles for the four HPG models (Table S7).

Most system states present with low ACTH with high GRD1 and GR1, or low LH/FSH with high GRD2 and

GR2, or low TEST/EST with high GRD3/4 and GR3/4, or with combinations of these, while all other state variables assume nominal values. This set of system states is the result of sensitivity to CORT introduced by the GR-GRD feedback loop. The states of the HPG-GR-HPGa model, based on the male HPG axis follow this regime exclusively, while the other 3 models based on the female HPG axis present with a variety of other states sharing a hypocortisolic characteristic. HPA-GR-HPG-GR models b and d show this hypocortisolic state when the HPG axis is suppressed in a model where it would normally promote the HPA axis. Model HPA-GR-HPGc however, only presents this low CORT state when the HPG axis is promoted. The multiplicity of system states that support a hypocortisolic condition is again due to the different combinations of activated or depressed GR and GRD in the regulatory network.

### 3.3 Immune Effects

Discrete representation of the simple immune system joined with the stand-alone HPA axis (Figure 3) produced 729 system states, and 2 stable steady states (Table S6): the nominal steady state (i.e. $\vec{x}(t) = (0,0,0,0,0,0)$), and a hypercortisolic condition with increased AIR and depressed IIR and IL-10 (i.e. $\vec{x}(t) = (0,0,1,1,-1,-1)$). Incorporating the GRD-GR loop in the model at the ACTH state variable on the HPA axis (Figure S5 A) generated 6561 system states, and yielded the above 2 stable steady states where all immune state variables were held at nominal values, and one additional state $\vec{x}(t) = (0,-1,0,1,1,0,0,0)$ (Table S6). The loss of the hypocortisolic state originally found in the HPG-GR model is due to multiple inputs to CORT, as also seen in the HPA-GR-HPG models. Adding the GR-GRD feedback loops to the IIR and the AIR (Figure S5 B) produced 531441 system states and 5 stable steady states (Table S6). However, the main characteristics of these states did not differ from the HPA-GR-Immune model as the additional states arose from the multiple combinations of activated GR5/6 and GRD5/6.

### 3.4 An Integrative Model

Combining the HPA axis with the HPG axis and immune system (Figure S6) produced 19683 system states. For HPG models a, b and d the steady state with all state variables at nominal value was produced, as well as a high CORT steady state with all levels of the HPG held low, high ADAP and low IIR and IL-10. HPA-

HPG-Immune model c yielded one additional state beyond these, with all levels of the HPA held low, all levels of the HPG high, and all levels of the immune system nominal (Table S8). Adding the HPG axis and immune components to the HPA-GR model (Figures 4 and S7) generated 177147 system states. HPA-GR-Immune-HPG models a, b, and d yielded 3 steady states (see Table S8). The first is the state with all variables at nominal levels, the second presents with low ACTH, high GR1 and GRD1, while the third corresponds to a hypercortisolic condition with high GR1, GRD1 and AIR, and a suppressed HPG axis, IIR and IL-10 concentration. HPA-GR-Immune-HPG model c presented 6 steady states, including the 3 discussed for the other models. The remaining 3 steady states showed low CRH, ACTH, and CORT, high GnRH, LH/FSH, and EST, nominal values for immune variables, and GRD1/GR1 state variables that cycled between low, nominal and high.

Previously, the addition of GR and GRD to the LH/FSH and TEST/EST variable nodes of the HPG circuit (Figures S8 and S9) resulted in different steady state profiles for the four different interaction models. This addition was investigated again with the addition of the immune system component. The HPA-GR-Immune-HPG-GR models produced 14348907 system states. Models a, b, and d of the HPG all produced 9 steady states with the same profile (Table S8), suggesting that the immune influence removes the variability between the models. Three general motifs were observed. The first motif, seen in 4 of the steady states, presents with a nominal state for HPA and immune variables, repressed LH/FSH and/or TEST/EST and increased levels of the accompanying GR and GRD. The second, which presented with nominal immune activation, low ACTH and high GR1 and GRD1, as well as repressed HPG nodes and increased HPG-related GR and GRD, accounted for another 4 steady states. The final steady state supported high CORT, GR1 and GRD1, low HPG along with high GR2/3/4 and GRD2/3/4, high AIR, and low IL-10 and IIR. Model c produced these same 9 steady states plus an additional 12 conditions all sharing a single motif of low CRH, ACTH and CORT, high GnRH, LH/FSH and EST, and nominal immune activation (Table S8). These 12 steady states are the result of GR1 and GRD1 again cycling between low, nominal and high values, and the HPG axis GR and GRD variables cycling between low and nominal value.

**3.5 Clinical Indicators of the GWI Steady State**

To validate these results the steroid and cytokine levels recorded in male Gulf War veterans with GWI and HCs were compared to the predicted steady states. At rest CORT levels in GWI veterans were found higher than normal with marginal significance ($p = 0.09$), whereas TEST levels at rest were found to be significantly lower ($p = 0.03$). The cytokines of the IIR in GWI patients were significantly decreased for IL-1a and 1L-1b ($p = 0.05$ and $0.04$, respectively), and significantly increased for IL-6 and IL-8 ($p = 0.03$ and $0.01$, respectively), while for the remaining majority of cytokines (IL-12p70, IL-15, IL-23 and TNF-$\alpha$) there was no significant change ($p > 0.10$). There was no significant difference in the expression of IL-10, used here as a mediating cytokine between the IIR and AIR state variable nodes ($p = 0.36$). For the cytokines belonging to the AIR aggregate set, GWI veterans showed a marginally significant increase in IL-2 ($p = 0.10$), a significant increase in IFN-$\gamma$ ($p = 0.02$), and a highly significant increase in IL-13 ($p < 0.01$). IL-4, IL-5 and TNF-$\beta$ did not show any significant changes between groups ($p > 0.10$).

Overall, the experimental results used here indicate that male GWI subjects present with low TEST, hypercortisolism, and an increased expression in the majority of cytokines related to the AIR. To compare against model predictions steroid and cytokine values found to be significantly higher in GWI patients were assigned a discrete value of 1, while those found to be significantly lower were valued at -1. Those showing no significant change were valued at 0. Experimental cytokine measurements were scored and aggregated into cytokine sets as described above. Comparison of these state variables showed a 40% match between GWI experimental data and the nominal SS0(HC) stable state predicted by the HPA-Immune-HPGa iteration of the model. In the case the predicted steady state SS2, described by low TEST, high CORT, high AIR values, there was a 60% match with experimental data for the GWI condition (Figure 5). While, the model shows a difference between the low ACTH, high GR1 and GRD1 steady state SS1 and the nominal steady state SS0(HC), the experimental markers do not allow for these states to be distinguished. Thus, measured endocrine-immune profiles for GWI show a 40% match with predicted steady state SS1.

### 3.6 Clinical Indicators of the CFS Attractor

Comparison of endocrine marker expression for female CFS patients and HCs showed significantly lower levels of CORT in blood ($p = 0.05$), and a marginally significant increase in EST levels ($p = 0.09$) for the

fatigued group.  Among cytokines belonging to the IIR set, levels of IL-8 were significantly lower in CFS

subjects  (p = 0.02), lower with high significance for IL-15 (p < 0.01), significantly higher for IL-1a and IL-1b

(p = 0.04, 0.02), and higher with high significance for IL-6 and IL-12p70 (p < 0.01). IL-23 and mediating

cytokine IL-10 showed no significant change.  Of the AIR cytokines, IL-4, IL-5 and TNF-$\beta$ all showed highly

significant elevations in expression (p < 0.01), whereas IL-13 levels were significantly lower in CFS (p =

0.01).  IFN-$\gamma$ and IL-2 showed no significant changes.

Taken together, experimental measurements indicated that female CFS patients presented with high EST,

hypocortisolism, and with a spectrum of altered cytokine levels. As in the case of GWI, the average

concentration of all cytokines falling within state variable set was rounded to the nearest integer and

projected onto a discrete scale. Comparison showed a 60% match between CFS experimental data and the

nominal (SS0(HC)) stable state predicted by the HPA-Immune-HPGc iteration of the model.  There is 0%

agreement with the low EST, high CORT and high AIR steady state SS2, which was found to closely

resemble the GWI profile.  However, there was a 100% match between measured levels of endocrine-

immune markers in CFS subjects and the high EST, low CORT, nominal immune steady states SS3, SS4

and SS5.  As there are no clinical markers to separate the SS3, SS4 and SS5 model states they are

referred to collectively (Figure 6).  As with GWI, the low ACTH, high GR1 and GRD1 steady state SS1 and

the nominal steady state SS0(HC), cannot be distinguished using the experimental data, and are also

considered collectively.  Thus, the measured CFS endocrine-immune profile showed a 60% match with

predicted steady state SS1.

**Discussion**

Multiple stable states are prime characteristics of systems displaying feedforward and feedback

mechanisms, and play a critical part in guiding the complex dynamics observed in biology.  Modeling these

complex systems can be quite challenging in the face of missing information regarding the stoichiometry

and in vivo kinetics in humans, however there is an abundance of connectivity data describing the "wiring"

of these biological circuits.  To make use of this wealth of information we have applied a discrete state

representation to the neuroendocrine immune system based solely on biological connectivity found in the

literature and a set of ternary logical rules. When this approach was applied to the conventional stand-alone HPA axis model the discrete state representation failed to produce multistability. This is consistent both with previous ordinary differential equation models [21-26] and the analysis of Thomas [29], which demonstrate that the presence of positive feedforward/feedback loops generates multiple stable states. Indeed, addition of the positive GR-GRD dimerization feedback loop generated a second stable state characterized by low ACTH, CORT and high GR-GRD. This is also consistent with the ordinary differential equation based models used by Gupta et al. [27] and Ben Zvi et al. [16]. Interestingly, when the GR-GRD feedback loop is added to the HPA axis in the HPA-HPG models, the original low CORT state found by Gupta et al. [27] disappears. This also occurred with the HPA-Immune model. This is a direct result of the state transition logic applied to the system. When multiple inputs determine the level of CORT all inputs must be low for CORT to drop, not just the level of ACTH as prescribed by Gupta et al. [27] and Ben Zvi et al. [16]. The hypocortisolic condition can be regained when neighboring regulatory systems are included, such as the female HPG axis. Thus, in simple models the GR-GRD loop is a necessary component to produce mutlistability, however in more complex regulatory circuits this feedback loop becomes redundant and is not required to produce multiple attractor states.

Gender appears to play an important role in supporting a hypocortisolic condition. Due to the suppressive actions of the male gonadal system in regulating itself and the HPA axis, a low CORT state is never available to the male, while the ability of the female sex hormone system to be both an inhibitor and/or activator readily supports the presence of a hypocortisolic condition. In the absence of the GR-GRD positive feedback loops on both the HPA and HPG axes, the female gonadal system is capable of generating a low CORT stable state, when the HPG axis inhibits the HPA axis while promoting itself. While literature suggests that this is a configuration that is available to the female gonadal system during a certain phase of the menstrual cycle, it remains to be confirmed experimentally. When the GR-GRD feedback loop is added to both the HPA and HPG axis multiple hypocortisolic states become available to the female in all wiring configurations save the case when the wiring is as shown for the male (i.e. the HPG inhibits both itself and the HPA). Interaction with the immune system also appears to play a significant role in determining abnormal CORT levels. While our models are very coarse grained in regard to the immune

system, they do suggest an important role for immune system feedback in sustaining hypercortisolic conditions. In our models CORT exerts a suppressive action on the IIR system while promoting the AIR. In turn, positive feedback by certain components of the immune system further elevates CORT levels leading to a hypercortisolic steady state. While, inclusion of the GR-GRD feedback loops on the HPA and immune system did yield additional steady states, it did not result in any significant changes to the profile in regards to CORT levels. The integrative model including the HPA and HPG axes and the simple immune system generates a hypercortisolic state in all 4 models of the HPG axis, and a hypocortisolic state only in model c of the HPG axis. The hypocortisolic states found in the HPA-GR-HPG-GR models are removed due to the presence of the stimulatory effects of the immune system on the HPA in all cases save for model c of the HPG. Again, the inclusion of the GR-GRD feedback loops on the HPA and HPG did yield additional steady states, but did not result in any significant changes to the system profiles.

These findings suggest that hypercortisolism is inextricably linked to an imbalance in the immune response. This is consistent with notions that GWI may be due to a systemic imbalance in immune signaling [51-53]. For example, Skowera et al. measured intracellular production of cytokines in peripheral blood and found ongoing Th1-type immune activation in symptomatic Gulf War Veterans compared to healthy counterparts [52]. More recent work confirms this finding while also suggesting that this may occur in the more complex context of a mixed Th1:Th2 response [51]. Additionally, Whistler et al. found evidence of innate immune involvement with GWI subjects exhibiting impaired immune function as characterized by decreased NK cytotoxicity, altered gene expression associated with NK cell function, altered pro-inflammatory cytokines, and T-cell ratios compared to control subjects [53]. This study also found dysregulated mediators of the stress response (including salivary cortisol) further suggesting a connection between altered cortisol levels and immune imbalance in GWI subjects. Conversely conditions involving hypocortisolism may be more strongly related to sex steroid suppression of the HPA axis and promotion of HPG function, a configuration seemingly available only to female subjects. This would suggest that the hypocortisolism seen in diseases, such as CFS [54-56], may be a result of the complexity afforded to the interaction between the HPA and HPG in female subjects, and may be an explanation for the reported prevalence of such diseases in women [57-62]. Indeed, these authors report that approximately 70% of observed CFS patients are women.

While certainly more comprehensive than their predecessors, these models remain relatively coarse representations of the interplay between the endocrine and immune systems. Misalignment with experimental data, in particular in the case of GWI, may stem from several limitations. First the discrete logic of the model is based on 3 states only making it impossible to distinguish between high and very high or low and very low. Misalignment may also be the result of missing interactions in the model regulatory network. The missing interactions may be located within the immune network itself, as immune cells have a complex crosstalk involving multiple cytokines [63]. However, the missing interactions may also involve systems that are not currently modeled, such as the role of key neurotransmitters linking the brain and central nervous system with the HPA axis and the immune system. For example, norepinephrine and epinephrine stimulate the $\beta_2$-adrenoreceptor-cAMP-protein kinase A pathway inhibiting the production of Th1/proinflammatory cytokines and stimulating the production of Th2/anti-inflammatory cytokines causing a selective shift from cellular to humoral immunity [64,65]. Additionally, lymphocytes express most of the cholinergic components found in the nervous system and may be stimulated by or release acetylcholine thus constituting a cholinergic system, separate from cholinergic nerves, that regulate immune function [66]. Similarly, as hypocortisolic diseases do not only occur in females the inability of our model to predict hypocortisolic states in males is an indication that low CORT states in males may be due to finer scale interactions between the HPA and HPG axes, or connections to other systems, such as the brain, that are not modeled here. As an example, neuropeptide Y, a molecule found in the nervous system that activates and stimulates the stress response, is not included in our model, but recently has been shown to play a role in CFS [67].

The simple models presented here illustrate the importance of an integrative approach to understanding complex illnesses. Further refinement of the model to include more detailed description of interactions within and between the HPA, HPG and immune systems could extend its applicability to other illnesses as would the incorporation of other key systems such as the brain and central nervous systems. Yet, even with the coarse-grained co-regulation networks investigated we found numerous stable resting states that differ significantly from normal and were indicative of complex and persistent regulatory imbalances. Findings

such as this support the use of an alternate model for disease, one which is not necessarily associated with failure of individual components, but rather with a shifts in their coordinated actions away from normal regulatory behavior. Response to exercise and other stressors has the potential to be very different in these new regulatory regimes. This is something that we have observed firsthand in our work with human GWI and CFS subjects [68]. As these models are based on currently documented knowledge of human physiology and regulatory biochemistry they are necessarily incomplete. They may nonetheless provide enough detail to identify simple and robust treatment avenues that would enable the body to recall its normal regulatory mode and naturally draw itself back into a more normal homeostasis.

**References**

1.      Groeneweg FL, Karst H, de Kloet ER, Joëls M (2011) Rapid non-genomic effects of corticosteroids and their role in the central stress response. J Endocrinol 209: 153–167.

2.      Lupien SJ, McEwen BS, Gunnar MR, Heim C (2009) Effects of stress throughout the lifespan on the brain, behaviour and cognition. Nat Rev Neurosci 10: 434-445.

3.      Mikics É, Kruk MR, Haller J (2004) Genomic and non-genomic effects of glucocorticoids on aggressive behavior in male rats. Psychoneuroendocrino 29:  618–635.

4.      Pariante CM, Lightman SL (2008) The HPA axis in major depression: classical theories and new developments.  Trend Neurosci 31: 464 – 468.

5.      Gerritsen L, Comijs HC, van der Graaf Y, Knoops AJ, Penninx BW, Geerlings MI (2011) Depression, hypothalamic pituitary adrenal axis, and hippocampal and entorhinal cortex volumes--the SMART Medea study. Biol Psychiatry 70: 373-380.

6.      Mehta D, Binder EB (2012) Gene × environment vulnerability factors for PTSD: The HPA-axis. Neuropharmacol 62: 654-662.

7.      Yehuda R (2009) HPA alterations in PTSD. In: Fink G, editor. Stress Consequences: Mental, Neuropsychological and Socioeconomic. San Diego: Academic Press. pp. 125-130.

8.      Young EA (2009) PTSD and HPA axis: same hormones, different disorders. In: Pariante CM, editor. Understanding Depression: A Translational Approach. New York: Oxford University Press. pp. 193-212.

9.      Gil-Bea FJ, Aisa B, Solomon A, Solas M, del Carmen Mugueta M, et al. (2010)  HPA axis dysregulation associated to apolipoprotein E4 genotype in Alzheimer's disease.  J Alzheimers Dis. 22: 829-838.

10.     Golier JA, Schmeidler J, Legge J, Yehuda R (2006) Enhanced cortisol suppression to dexamethasone associated with Gulf War deployment. Psychoneuroendocrinology 31(10): 1181-1189.

11.     Golier JA, Schmeidler J, Legge J, Yehuda R (2007) Twenty-four hour plasma cortisol and adrenocorticotropic hormone in Gulf War Veterans: relationships to posttraumatic stress disorder and health symptoms. Biol Psychiatry 62(10): 1175–1178.

12.     Golier JA, Schmeidler J, Yehuda R (2009) Pituitary response to metyrapone in Gulf War veterans: relationship to deployment, PTSD and unexplained health symptoms. Psychoneuroendocrinology 34(9): 1338-1345. E

13.     Van Den Eede F, Moorkens G, Van Houdenhove B, Cosyns P, Claes SJ (2007) Hypothalamic-pituitary-adrenal axis function in chronic fatigue syndrome. Neuropsychobiol 55: 112–120.

14.     Crofford LJ, Young EA, Engleberg NC, Korszun A, Brucksch CB, et al. (2004) Basal circadian and pulsatile ACTH and cortisol secretion in patients with fibromyalgia and/or chronic fatigue syndrome. Brain Behav Immun 18: 314–325.

15.     Aschbacher K, Adam EK, Crofford LJ, Kemeny ME, Demitrack MA, et al. (2012) Linking disease symptoms and subtypes with personalized systems-based phenotypes: A proof of concept study. Brain Behav Immun. In Press.

16.     Ben-Zvi A, Vernon SD, Broderick G (2009) Model-Based Therapeutic Correction of Hypothalamic-Pituitary-Adrenal Axis Dysfunction. PLoS Comp Biol 5: e1000273.

17.     Alon U. Network motifs: theory and experimental approaches. Nat Rev Genet. 2007 Jun;8(6):450-61. Review.

18.     Lightman SL, Conway-Campbell BL (2010) The crucial role of pulsatile activity of the HPA axis for continuous dynamic equilibration, Nat Rev Neurosci 11: 710-718.

19.     Bairagi N, Chatterjee S, Chattopadhyay J (2008) Variability in the secretion of corticotropin-releasing hormone, adrenocorticotropic hormone and cortisol and understandability of the hypothalamicpituitary-adrenal axis dynamics--a mathematical study based on clinical evidence. Math Med Biol 25: 37–63.

20. Kyrylov V, Severyanova LA, Vieira A (2005) Modeling robust oscillatory behavior of the hypothalamic-pituitary-adrenal axis. IEEE Trans Biomed Eng 52: 1977–1983.

21. Savic D, Jelic S (2005) A theoretical study of hypothalamo-pituitary adrenocortical axis dynamics. Ann NY Acad Sci 1048: 430–432.

22. Savic D, Jelic S (2005) A mathematical model of the hypothalamopituitary-adrenocortical system and its stability analysis. Chaos Solitons Fractals 26: 427–436.

23. Lenbury Y, Pornsawad P (2005) A delay-differential equation model of the feedback-controlled hypothalamus-pituitary-adrenal axis in humans. Math Med Biol 22: 15–33.

24. Gonzalez-Heydrich J, Steingard RJ, Kohane I (1994) A computer simulation of the hypothalamic-pituitary-adrenal axis. Proc Annu Symp Comput Appl Med Care 1994: 1010.

25. Dempsher DP, Gann DS, Phair RD (1984) A mechanistic model of ACTH-stimulated cortisol secretion. Am J Physiol 246: R587-R596.

26. Sharma DC, Gabrilove JL (1975) A study of the adrenocortical disorders related to the biosynthesis and regulation of steroid hormones and their computer simulation. Mt Sinai J Med 42: S2-S39.

27. Gupta S, Aslakson E, Gurbaxani BM, Vernon SD (2007) Inclusion of the glucocorticoid receptor in a hypothalamic pituitary adrenal axis model reveals bistability. Theor Biol  Med Model 4: 8.

28. Thomas R, Thieffry D, Kaufman M (1995) Dynamical behaviour of biological regulatory networks--I. Biological role of feedback loops and practical use of the concept of the loop-characteristic state. Bull Math Biol. 57: 247-276.

29. Thomas R (1991) Regulatory Networks Seen as Asynchronous Automata: A Logical Description. J Theor Biol 153: 1-23.

30. Mendoza L, Xenarios I (2006) A method for the generation of standardized qualitative dynamical systems of regulatory networks Theor Biol Med Model 3: 13.

31.    Keller-Wood ME, Dallman MF (1984) Corticosteroid inhibition of ACTH secretion. Endocrinol Rev 5: 1–24.

32.    Viau V (2002) Functional Cross-Talk Between the Hypothalamic-Pituitary-Gonadal and -Adrenal Axes. J Neuroendocrinol 14: 506–513.

33.    Dallman MF, Viau V, Bhatnagar S, Laugero K, Gomez F, et al. (2002) Corticotropin-releasing factor (CRF), corticosteroids and stress, energy balance, the brain and behavior. In: Pfaff DW, editor. Hormones, Brain and Behavior. New York: Academic Press. Pp. 571-632.

34.    Tilbrook AJ, Turner AI, Clarke IJ (2000) Effects of stress on reproduction in non-rodent mammals: the role of glucocorticoids and sex differences. Rev Reprod 5: 105–113.

35.    Torpy DJ, Chrousos GR (1996) The three-way interactions between the hypothalamic-pituitary-adrenal and gonadal axes and the immune system. Baillires Clin Rheumatol 10: 181-198.

36.    Rivier C, Rivest S (1991) Effect of stress on the activity of the hypothalamic pituitary-gonadal axis: peripheral and central mechanisms. Biol Reprod 45: 523–532.

37.    Piñón R (2001) Biology of human reproduction. Sausalito: University Science Books. 535 p.

38.    Silverman MN, Pearce BD, Biron CA, Miller AH (2005) Immune modulation of the hypothalamic-pituitary-adrenal (HPA) axis during viral infection. Viral Immunol 18: 41-78.

39.    Cutolo M (2004) Immune System, Hormonal Effects on. In: Martini L, editor. Encyclopedia of Endocrine Diseases, Volume 2. Elsevier Academic Press. pp. 755-760.

40.    Berczi I, Szentivanyi A (2003) Autoimmune disease. In: Berczi I, Szentivanyi A, editors. Neuroimmmune Biology: Vol. 3: The Immune-Neuroendocrine Circuitry. History and Progress. Amsterdam: Elsevier Science BV. pp. 495-536

41.    Saraiva M, O'Garra A (2010) The regulation of IL-10 production by immune cells. Nat Rev Immunol 10: 170-181.

42. Elenkov IJ (2004) Glucocorticoids and the Th1/Th2 balance. Ann NY Acad Sci 1024: 138-146.

43. Vernon SD, Reeves WC (2006) The challenge of integrating disparate high-content data: epidemiological, clinical and laboratory data collected during an in-hospital study of chronic fatigue syndrome. Pharmacogenomics 7: 345–354.

44. Reeves WC, Wagner D, Nisenbaum R, Jones JF, Gurbaxani B, et al. (2005) Chronic fatigue syndrome — a clinically empirical approach to its definition and study. BMC Med 3: 19.

45. Fuite J, Vernon SD, Broderick G (2008) Neuroendocrine and immune network re-modeling in chronic fatigue syndrome: An exploratory analysis. Genomics 92: 393–399.

46. Broderick G, Craddock RC, Whistler T, Taylor R, Klimas N, et al. (2006) Identifying illness parameters in fatiguing syndromes using classical projection methods. Pharmacogenomics 7: 407–419.

47. Reeves WC, Lloyd A, Vernon SD, Klimas N, Jason LA, et al. (2003) Identification of ambiguities in the 1994 chronic fatigue syndrome research case definition and recommendations for resolution. BMC Health Serv Res 3: 25.

48. Fukuda K, Nisenbaum R, Stewart G, Thompson WW, Robin L, et al. (1998) Chronic multisymptom illness affecting Air Force veterans of the Gulf War. J Am Med Assoc 280: 981–998.

49. Broderick G, Fuite J, Kreitz A, Vernon SD, Klimas N, et al. (2010) A formal analysis of cytokine networks in Chronic Fatigue Syndrome. Brain Behav Immun 24: 1209-1217.

50. Collins JF, Donta ST, Engel CC, Baseman JB, Dever LL, et al. (2002) The antibiotic treatment trial of Gulf War Veterans' Illnesses: issues, design, screening, and baseline characteristics. Control Clin Trials 23: 333–353.

51. Broderick G, Kreitz A, Fuite J, Fletcher MA, Vernon SD, et al. (2011) A pilot study of immune network remodeling under challenge in Gulf War Illness. Brain Behav Immun 25: 302–313.

52. Skowera A, Hotopf M, Sawicka E, Varela-Calvino R, Unwin C et al. (2004) Cellular Immune Activation in Gulf War Veterans. J Clin Immunol 24: 66-73.

53. Whistler T, Fletcher MA, Lonergan W, Zeng XR, Lin JM, et al. (2009) Impaired immune function in Gulf War Illness. BMC Medical Genomics 2: 12.

54. Papadopoulos AS, Cleare AJ (2012) Hypothalamic–pituitary–adrenal axis dysfunction in chronic fatigue syndrome. Nat Rev Endocrinol 8: 22-32

55. Jerjes WK, Peters TJ, Taylor NF, Wood PJ, Wessely S, et al. (2006) Diurnal excretion of urinary cortisol, cortisone, and cortisol metabolites in chronic fatigue syndrome. Psychosom Res 60: 145–153.

56. Cleare AJ (2003) The neuroendocrinology of chronic fatigue syndrome. Endocr Rev 24: 236–252.

57. Nacul LC, Lacerda EM, Pheby D, Campion P, Molokhia M, et al. (2011) Prevalence of myalgic encephalomyelitis/chronic fatigue syndrome (ME/CFS) in three regions of England: a repeated cross-sectional study in primary care. BMC Med 9: 91.

58. Evengard B, Jacks A, Pedersen N, Sullivan PF (2005) The epidemiology of chronic fatigue in the Swedish Twin Registry. Psych Med 35: 1317-1326.

59. Gallagher AM, Thomas JM, Hamilton WT, White PD (2004) Incidence of fatigue symptoms and diagnoses presenting in UK family care from 1990 to 2001. J Roy Soc Med 97: 571-575.

60. Reyes M, Nisenbaum R, Hoaglin D, Unger ER, Emmons C, et al. (2003) Prevalence and incidence of chronic fatigue syndrome in Wichita, Kansas. Arch Intern Med 163: 1530-1536.

61. Lindal E, Stefansson JG, Bergmann S (2002) The prevalence of chronic fatigue syndrome in Iceland—a national comparison by gender drawing on four different criteria. Nord J Psychiatry 56: 273-277. Erratum in: Lindal E, Stefansson JG, Bergmann S (2006) Nord J Psychiatry. 60: 183.

62. Jason LA, Richman JA, Rademaker AW, Jordan KM, Plioplys AV, et al. (1999) A community-based study of chronic fatigue syndrome. Arch Intern Med 159: 2129-2137.

63. Frankenstein Z, Alon U, Cohen IR (2006) The immune-body cytokine network defines a social architecture of cell interactions. Biol Direct 1: 32.

64.     Kin NW, Sanders VM (2006) It takes nerve to tell T and B cells what to do. J Leukocy Biol 79: 1093-1104.

65.     Elenkov IJ, Wilder RL, Chrousos GP, Vizi ES (2000) The Sympathetic Nerve—An Integrative Interface between Two Supersystems: The Brain and the Immune System. Pharmacol Rev 52: 595-638.

66.     Kawashima K, Fujii T (2003) The lymphocytic cholinergic system and its contribution to the regulation of immune activity. Life Sci 74: 675–696.

67.     Fletcher MA, Rosenthal M, Antoni M, Ironson G, Zeng XR, et al. (2010). Plasma neuropeptide Y: a biomarker for symptom severity in chronic fatigue syndrome. Behav Brain Funct. 6: 76.

68.     Broderick G, Fletcher MA, Gallgher M, Barnes Z, Vernon SD, et al. (2012) Exploring the Predictive Potential of Immune Response to Exercise in Gulf War Illness. In: Yan Q. (Ed.), Psychoneuroimmunology: Methods and Protocols (Methods in Molecular Biology), Springer, New York, NY, In Press

**Figure 1:** The stand-alone HPA models. (A) HPA model. (B) HPA-GR model.

**Figure 2:** The HPA-HPG models. (A) HPA-HPGa. (B) HPA-HPGb. (C) HPA-HPGc. (D) HPA-HPGd.

**Figure 3:** The HPA-Immune model.

**Figure 4:** The HPA-GR-Immune-HPG-GR models. (A) HPA-GR-Immune-HPGa-GR. (B) (B) HPA-GR-Immune-HPGc-GR. Note: HPA-GR-Immune-HPGb-GR and HPA-GR-Immune-HPGd-GR may be found in supplementary information Figure S7.

**Figure 5:** Clinical indicators of the GWI attractor. Comparison of HPA-GR-Immune-HPGa model steady states with male GWI clinical data expressed in terms of model nodes.

**Figure 6:** Clinical indicators of the CFS attractor. Comparison of HPA-GR-Immune-HPGc model steady states with female CFS clinical data expressed in terms of model nodes.

**Table 1:** Steady States of Key HPA-axis models.  White – nominal state (0); Green – high state (1); Red – low state (-1); Grey – N/A to the model)

| Model # | CRH | ACTH | CORT | GRD1 | GR1 | GnrH | LH/FSH | TEST | EST | AIR | IIR | IL-10 |
|---|---|---|---|---|---|---|---|---|---|---|---|---|
| HPA | 0 | 0 | 0 | N/A | N/A | N/A | N/A | N/A | N/A | N/A | N/A | N/A |
| HPA-GR | 0 | -1 | -1 | 1 | 1 | N/A | N/A | N/A | N/A | N/A | N/A | N/A |
| HPA-GR-Immune-HPGa | 0 | -1 | 0 | 1 | 1 | -1 | -1 | N/A | 0 | 1 | -1 | -1 |
| HPA-GR-Immune-HPGb | 0 | -1 | 0 | 1 | 1 | -1 | -1 | N/A | 0 | -1 | -1 | -1 |
| HPA-GR-Immune-HPGc | -1 | -1 | 0 | 1 | 1 | -1 | 0 | N/A | 1 | 0 | 0 | 0 |
| HPA-GR-Immune-HPGd | 0 | -1 | 0 | 1 | 1 | -1 | -1 | N/A | -1 | 1 | -1 | -1 |

46

# Figure 1



# Figure 2

# Figure 3



# Figure 4

**A**



**B**
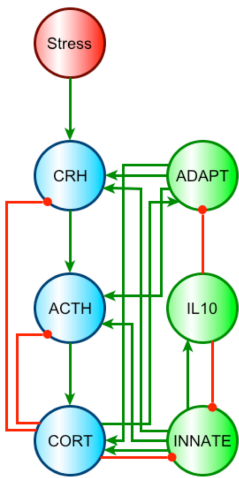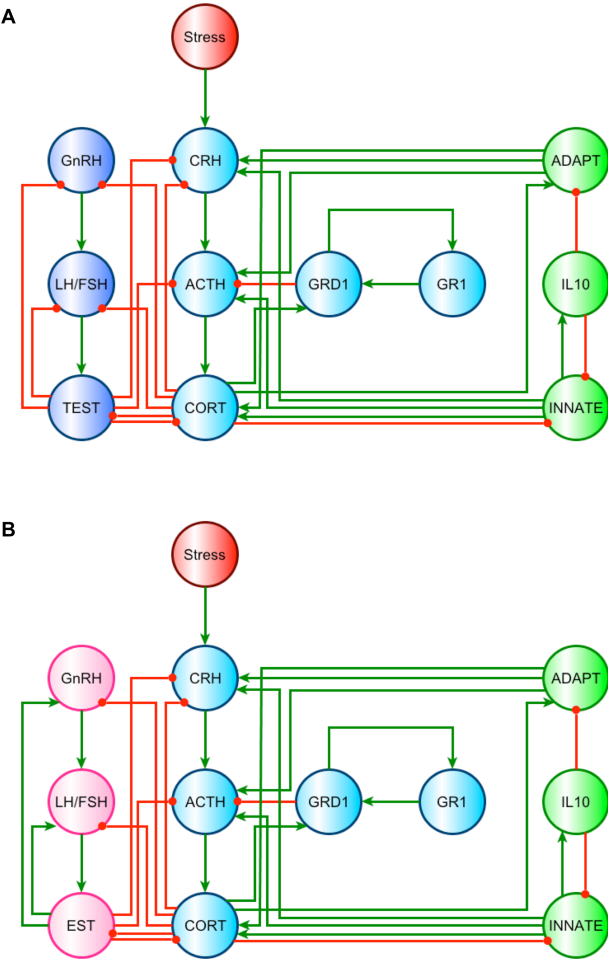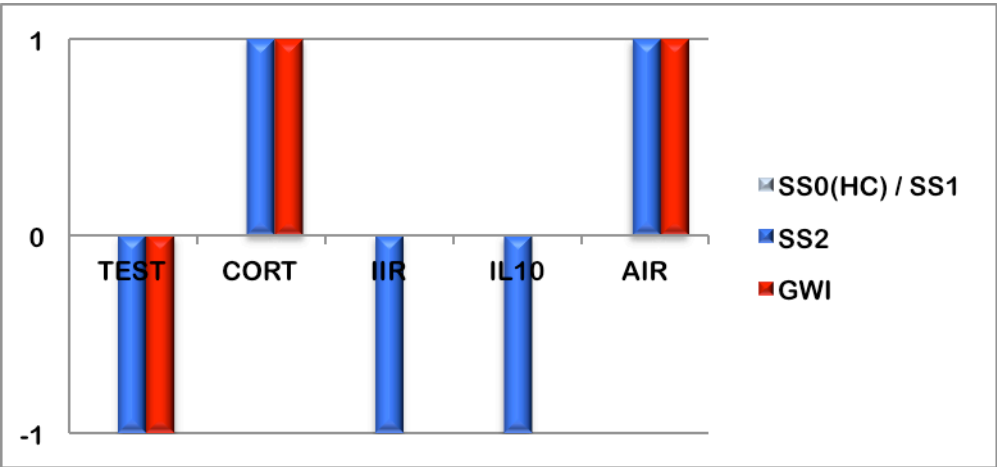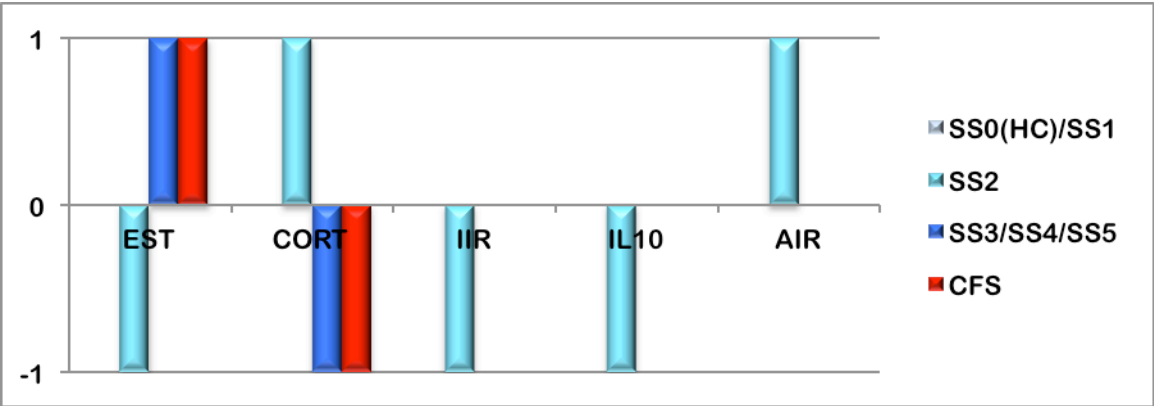
Figure 5



Figure 6

**Appendix B**:

Excerpts from Methods section, Tables and Figures from:

Fritsch P, Craddock TJA, Smylie AL, Folcik Nivar VA, Fletcher MA, Klimas NG, de Vries G, Broderick G. A Study of Multiple Homeostatic Regimes in a Discrete Logic Model of Immune Signaling. 2012. *In preparation*.

**A Study of Multiple Homeostatic Regimes in a Discrete Logic Model of Endocrine-Immune Networks**.

Paul Fritsch [a], Travis J.A. Craddock [a], Anne Liese Smylie [a], Virginia A. Folcik Nivar [b], Mary Ann Fletcher [c], Nancy G Klimas [d], Gerda de Vries [e], Gordon Broderick [a: 1]

[a] Department of Medicine, University of Alberta, Edmonton, Canada

Ph: +1- 780-232-9312      Email: pfritsch@ualberta.ca

Ph: +1- 780-552-3894      Email: travisc@ualberta.ca

Ph: +1- 780-250-2784      Email: smylie@ualberta.ca

Ph: +1-780-492-1633      Email: gordon.broderick@ualberta.ca

[b] Department of Internal Medicine, Ohio State University Medical Center, Columbus, OH

Ph: +1- 614-366-1332      Email: Virginia.Nivar@osumc.edu

[c] Department of Medicine, University of Miami, Miami, FL

Ph: +1- 305-243-6525      Email: MFletche@med.miami.edu

[d] Department of Medicine, Nova Southeastern University, Fort Lauderdale, FL

Ph: +1- 305-575-3267      Email: nklimas@nova.edu

[e] Department of Math. & Stat. Sci., University of Alberta, Edmonton, Canada

Ph: +1- 780-492-4561      Email: devries@math.ualberta.ca

[1] Corresponding author:  Dr. Gordon Broderick, Associate Professor

Div. of Pulmonary Medicine, Dept. of Medicine, University of Alberta

WMC 2E4.41 WC Mackenzie Health Sciences Centre

8440 - 112 Street, Edmonton AB T6G 2R7, Canada

Ph: +780.492.1633   Fax: +780.407.3027   email: gordon.broderick@ualberta.ca

Excerpt from **<u>Methods</u>**

*A Theoretical Immune Signaling Network*

Based on the work of Folcik *et al.* (2011), a wiring diagram was constructed for the interactions between immune cells and their cytokines [Figure 1]. Cytokines under consideration in this study include interleukin (IL)-1, IL-2, IL-4, IL-5, IL-6, IL-8, IL-10, IL-12, IL-13, IL-23, IL-27, interferon (IFN)-$\gamma$, and tumor necrosis factor (TNF)-$\alpha$. Because of the great number of cytokines utilized by the immune system, some of these cytokines must be grouped together into a single node so as not to exceed computational limitations. In accordance with Folcik *et al.* (2011), cytokines were grouped into either a monokine (MK) or cytokine (CK) group. MKs represent the cytokines released primarily by the monocytes (DCs) and CKs represent the cytokines released by the lymphocytes (NK cells, Th cells, and CTLs). MK1 and CK1 are pro-inflammatory cytokine groupings, whereas MK2 and CK2 are anti-inflammatory cytokine groupings. See Table 4 for the cytokine groupings used. It should be noted that the MK2 node can also represent the anti-inflammatory dendritic cells, however, since these dendritic cells have only one input (Infection) and only one output (MK2), these 2 nodes can be compressed into a single node consisting of the MK2 cytokines.

Although most of the immune cells exhibit numerous levels of activation, since they will eventually convert to a state where they release the cytokines of interest, they can be condensed into a single node, capable of being downregulated (-1), nominal (0), or upregulated (1). For example, Th1 cells start as naïve germ cells, which differentiate to various levels of effector cells. Effector cells release cytokines or mature into memory cells. Since we are only concerned with the cytokines these cells release, a single node can represent all activation levels of Th1 cells.

Even though Folcik *et al.* (2011) includes macrophages, Tregs, B cells, and Th17 cells in their model, these cells were not essential in attaining any additional or interesting stable attractor states. For example, B cells primarily release types of immunoglobulins (antibodies), which are not measured in the patient cohorts for GWI and CFS. Therefore, including B cells in this model would not enhance the potential alignment with the clinical data. Also, some of these cell populations included by Folcik *et al.* (2011) do not have a substantial feedback role with the majority of the immune response. For example, Th17 cells release

predominantly IL-17, which does not exert significant feedback on the other immune cells included in this model.

Next, the hormonal inputs of cortisol and testosterone were added to the wiring diagram [Fig 2]. Cortisol acts to suppress NK cell activity (Bush *et al.,* 2012), Th1 activity (Liberman *et al.,* 2009), and inflammatory DC activity (Zen *et al.,* 2011). Cortisol also has an effect on Th2 cells, but in a more indirect way than the other cells previously mentioned. Cortisol acts on naïve T-cells to repress both the Th1 promoting transcription factor, T-bet, and the Th2 promoting transcription factor, GATA-3, although the suppressive effect on T-bet is much stronger than the suppressive effect on GATA-3. Therefore, if T-cells are already committed to differentiating, a Th2 favored shift in T-cell development is observed with long-term exposure to cortisol, which can be characteristic in chronic illnesses (Liberman *et al.,* 2009). Consequently, cortisol is assumed to have a promoting effect on Th2 cells.

It has also been demonstrated that the pro-inflammatory cytokines, predominantly IL-1, IL6, and TNF-$\alpha$, activate the HPA axis at the hypothalamic level by inducing CRH secretion consequently leading to increased release of ACTH and eventually cortisol (Cutolo, 2004).

In regards to the male HPG axis effects on the immune system, studies have shown that testosterone and other androgens exert a suppressive effect on the IL-6 gene, thereby decreasing its synthesis (Cutolo, 2004). Testosterone also acts to enhance the Th1 response and activate CTLs (González *et al.*, 2010). Cytokines can also exert negative feedback on the male HPG axis. It has been shown that receptors for the pro-inflammatory cytokines, IFN-$\gamma$ and TNF-$\alpha$, exist on male leydig cells and act to decrease the production of testosterone. As well, TNF-$\alpha$ has been shown to decrease the release of GnRH in the hypothalamus and LH in the pituitary gland eventually causing a decrease in testosterone levels (Foster *et al.,* 2003).

Not only is there cross talk between hormonal axes and the immune system, but also between the hormonal axes. For example, the HPA and the HPG axes have a negative effect on each other. It has been observed that testosterone, via its androgen receptor, will inhibit the higher levels of the HPA axis (Viau,

2002). Furthermore, cortisol has been shown to suppress the HPG axis, inhibit the effects of testosterone, and downregulate androgen receptor expression (Mehta and Josephs, 2010).

From this more completely represented diagram, we can write out the image vectors,          , for each node [Table 5]. An in-house Python script was used to analyze this state network.

*Discrete Encoding of Clinical Data*

Once the simulation returns the stable attractor states, the predicted states are compared against clinical data for GWI and CFS. Using a cohort of 27 GWI affected males, 17 CFS affected males, and 29 healthy control males, cytokine levels were measured at rest in IL-12, IL-1a, IL-1b, IL-8, IL-10, IL-4, IL-6, IL-23, IFN-$\gamma$, IL-2, TNF-$\alpha$, IL-5, and IL-13. Levels of cortisol and testosterone were also measured in these cohorts. Note that only cytokine levels are being compared because data on cell populations was not available from the cohort data. Also, the node MK27 was not included in this comparison because levels of IL-27 were not included in this study. The log base 2 transform of this data was taken and the average value of these log transforms was recorded for each cohort. A one tailed t-test was performed to ascertain whether there is a significant increase or decrease in cytokine or hormone levels between healthy controls and GWI or CFS men. Ternary values are assigned to each cytokine based on their p-values. If the relative levels of cytokines in GWI or CFS patients are found to be insignificantly different from those recorded in the healthy control (p-value>0.10), a ternary value of 0 is assigned in order to match the model's ternary system. If the relative levels of cytokines in GWI or CFS patients are found to be significantly different from those recorded in the healthy control (p-value ≤0.10), a ternary value of -1 or 1 is assigned based on the relative difference between the log transformed means of GWI or CFS patients' cytokines/hormones and healthy controls' cytokines/hormones. For instance, if the log transformed mean of the GWI/CFS patients' cytokines/hormones is higher than the log transformed mean of the healthy controls' cytokines/hormones and significance is found (p-value ≤0.10), then a value of 1 is assigned to that node. As well, if the log transformed mean of the GWI/CFS patients' cytokines/hormones is lower than the log transformed mean of the healthy controls' cytokines/hormones and significance is found (p-value ≤0.10), then a value of -1 is assigned to that node [this data is summarized in table 6 for GWI and in table 7 for CFS]. Since groups of

cytokines are modeled instead of individual cytokines (ie MK1, MK2, CK1, and CK2), the ternary values represented by the individual cytokines must be aggregated into one ternary value representing the groups of cytokines. Taking the average of the ternary values for each cytokine or hormone within the grouped nodes and then rounding that value to the nearest integer represents the overall ternary value for that node in the model [Table 8]. These numbers are used for comparison between clinical data and the predicted values of the model.

References

Ackerman, L.S. (2006) Sex Hormones and the Genesis of Autoimmunity. *Archives of Dermatology*. 142: 371-376.

Broderick, G., Fuite, J., Kreitz, A., Vernon, S.D., Klimas, N., and Fletcher, M.A. (2010) A formal analysis of cytokine networks in Chronic Fatigue Syndrome. *Brain Behavior and Immunity.* 24: 1209-1217.

Broderick, G., Kreitz, A., Fuite, J., Fletcher, M.A., Vernon, S.D., and Klimas, N. (2011) A pilot study of immune network remodeling under challenge in Gulf War Illness. *Brain Behavior and Immunity.* 25: 302-313.

Bush, K.A., Krukowski, K., Eddy, J.L., Janusek, L.W., and Mathews, H.L. (2012) Glucocorticoid receptor mediated suppression of natural killer cell activity: Identification of associated deacetylase and corepressor molecules. *Cellular Immunology.* 275:80-89.

Cutolo, M., Seriolo, B., Villaggio, B., Pizzorni, C., Craviotto, C., and Sulli, A. (2002) Androgens and Estrogens Modulate the Immune and Inflammatory Reponses in Rheumatoid Arthritis. *Annals of the New York Academy of Sciences.* 966: 131-142.

Cutolo, M. (2004) Immune System, Hormonal Effects on. *Encyclopedia of Endocrine Diseases.* 2:755-760.

Diehl, S. and Rincón, M. (2002) The two faces of IL-6 on Th1/Th2 differentiation.  *Molecular Immunology.* 39: 531-536.

Djurhuus, C.B., Gravholt, C.H., Nielsen, S., Mengel, A., Christiansen, J.S., Schmitz, O.E., and Moller, N. (2002) Effects of cortisol on lipolysis and regional interstitial glycerol levels in humans. *American Journal of Physiology. Endocrinology and Metabolism.* 283: E172-E177.

Elenkov, I.J., Wilder, R.L., Chrousos, G.P., and Vizi, E.S. (2000) The Sympathetic Nerve- An Integrative Interface Between Two Supersystems: The Brain and the Immune System. *Pharmacological Reviews.* 52: 595-638.

Folcik, V.A., Broderick, G., Mohan, S., Block, B., Ekbote, C., Doolittle, J., Khoury, M., Davis, L., and Marsh, C.B. (2011) Using an agent based model to analyze the dynamic communication network of the

immune response. *Theoretical Biology and Medical Modeling*. 8:1-25.

Foster, S., Daniels, C., Bourdette, D., and Bebo, B.F. (2003) Dysregulation of the hypothalamic-pituitary-gonadal axis in experimental autoimmune encephalomyelitis and multiple sclerosis. *Journal of Neuroimmunology.* 140: 78-87.

Frankenstein, Z., Alon, U., and Cohen, I.R. (2006) The immune-body cytokine network defines a social architecture of cell interactions. *Biology Direct.* 1:32.

Fukuda, K., Nisenbaum, R., Stewart, G., Thompson, W.W., Robin, L., Washko, R.M., Noah, D.L., Barrett, D.H., Randall, B., Herwaldt, B.L., Mawle, A.C., and Reeves, W.C. (1998) Chronic Multisymptom Illness Affecting Air Force Veterans of the Gulf War. *Jounal of the American Medical Association*. 280: 981-988.

González, D., Díaz, B., Pérez, M., Hernández, A., Chico, B., and León, A. (2010) Sex hormones and autoimmunity. *Immunology Letters.* 133: 6-13.

Hodkinson, C.F., Simpson, E.E.A., Beattie, J.H., O'Connor, J.M., Campbell, D.J., Strain, J.J., and Wallace, J.M.W. (2009) Preliminary evidence of immune function modulation by thyroid hormones in healthy men and women aged 55–70 years. *Journal of Endocrinology.* 202: 55-63.

Kalinski, P. and Moser M. (2005) Consensual immunity: success driven development of T-helper 1 and T-helper 2 responses. *Nature Reviews. Immunology.* 5: 251-260.

Kamiya, S., Okumura, M., Chiba, Y., Fukawa, T., Nakamura, C., Nimura, N., Mizuguchi, J., Wada, S., and Yoshimoto, T. (2011) IL-27 supresses RANKL expression in CD4+ T cells in part through STAT3. *Immunology Letters*. 138: 47-53.

Kang, H.K., Natelson, B.H., Mahan, C.M., Lee, K.Y., and Murphy, F.M. (2003) Post-traumatic stress disorder and chronic fatigue syndrome-like illness among Gulf War veterans: a population-based survey of 30,000 veterans. *American Journal of Epidemiology.* 157: 141-148.

Kawashima, K. and Fujii, T. (2003) The lymphocytic cholinergic system and its contribution to the regulation

of immune activity. *Life Sciences.* 74: 675-696.

Liberman, A.C., Druker, J., Refojo, D., Holsboer, F., and Arzt, E. (2009) Glucocorticoids inhibit GATA-3 phosphorylation and activity in T cells. *Federation of American Societies for Experimental Biology (FASEB) Journal.* 23: 1558-1571.

Mehta, P.H. and Josephs, R.A. (2010) Testosterone and cortisol jointly regulate dominance: Evidence for a dual-hormone hypothesis. *Hormones and Behavior.* 58: 898-906.

Mendoza, L. and Xenarios, I. (2006) A method for the generation of standardized qualitative dynamical systems of regulatory networks. *Theoretical Biology and Medical Modeling*. 3: 13.

Mills, K.H. (2011) TLR dependent T cell activationin autoimmunity. *Nature Reviews. Immunology.* 11: 807-822.

O'Garra, A., Vieira, P.L., Vieira, P., and Goldfeld, A.E. (2004) IL-10 producing and naturally occurring CD4^{+} Tregs: limiting collateral damage. *The Journal of Clinical Investigation.* 114: 1372-1378.

Orosz, C.G. (2002) The Case for Immuno-Informatics. *Graft.* 5: 462-465.

Pavlov, V.A., and Tracey, K.J. (2005) The cholinergic anti-inflammatory pathway. *Brain Behavior and Immunity*. 19: 493-499.

Riad, M., Mogos, M., Thangathurai, D., and Lumb, P.D. (2002) Steroids. *Current opinion in critical care.* 8: 281-284.

Sia, Charles (2005) Imbalance in Th Cell Polarization and its Relevance in Type 1 Diabetes Mellitus. *The Review of Diabetic Studies.* 2:182-186.

Silverman, M.N., Pearce, B.D., Biron, C.A., and Miller A.H. (2005) Immune Modulation of the Hypothalamic-Pituitary-Adrenal (HPA) Axis during Viral Infection. *Viral Immunology.* 18: 41-78.

Simmons, P.S., Miles, J.M., Gerich, J.E., and Haymond, M.W. (1984) Increased proteolysis. An effect of increases in plasma cortisol within physiologic range. *Journal of Clinical Investigation.* 73: 412-420.

Simpson, C.R., Anderson, W.J.A., Helms, P.J., Taylor, M.W., Watson, L., Prescott, G.J., Godden, D.J., and Barker, R.N. (2002) Coincidence of immune-mediated diseases driven by Th1 and Th2 subsets suggests a common aetiology. A population-based study using computerized General Practice data. *Clinical and Experimental Allergy: journal of the British Society for Allergy and Clinical Immunology.* 32: 37-42.

Stadler, P.F., Schuster, P., and Perelson, A.S. (1994) Immune networks modeled by replicator equations. *Journal of Mathematical Biology.* 33: 111-137.

Thomas, Rene (1991) Regulatory Networks Seen as Asynchronous Automata: A Logical Description. *Journal of Theoretical Biology.* 153:1-23.

Viau, V. (2002) Functional Cross-Talk Between the Hypothalamic-Pituitary-Gonadal and -Adrenal Axis. *Journal of Neuroendocrinology*. 14: 506-513.

Warnatz, K. and Voll, R.E. (2012) Pathogenesis of autoimmunity in common variable immunodeficiency. *Frontiers in Immunology.* 3: 210.

Wheway, J., Mackay, C.R., Newton, R.A., Sainsbury, A., Boey, D., Herzog, H., and Mackay, F. (2005) A fundamental bimodal role for NPY Y1 receptor in the immune system. *Journal of Experimental Medicine.* 202: 1527-1538.

Wolfe, J., Proctor, S.P., Davis, J.D., Borgos, M.S., and Friedman, M.J. (1998) Health Symptoms Reported by Persian Gulf War Veterans Two Years After Return. *American Journal of Industrial Medicine.* 33: 104-113.

Zen, M., Canova, M., Campana, C., Bettio, S., Nalotta, L., Rampudda, M., Ramonda, R., Iaccarino, L., and Doria, A. (2011) The kaleidoscope of glucocorticoid effects on immune system. *Autoimmunity Reviews.* 10: 305-310.

**Figure 1:** Wiring Diagram of the interactions between innate cells (yellow), adaptive cells (orange), and the cytokines they produce (blue). The Infection node (grey) is a necessary component of the program, but was kept consistently nominal so it would have no effect on the overall network as per the logical function. Green connections indicate an activating influence and red connections indicate an inhibiting influence.

**Figure 2:** Wiring Diagram for the immune network with hormonal inputs from cortisol and testosterone (purple). The nodes, Stress, Infection, and Male HPG axis (grey) were necessary components of the program required as inputs, but they were kept consistently nominal so they would have no effect on the overall network as per the logical functions. Green connections indicate an activating influence and red connections indicate an inhibiting influence.

**Figure 3**: Steady state 1 (SS1) as predicted by the simulation. Baseline refers to a value of 0, above baseline refers to a value of 1, and below baseline refers to a value of -1.

**Figure 4:** Steady State 2 (SS2) as predicted by the simulation. Baseline refers to a value of 0, above baseline refers to a value of 1, and below baseline refers to a value of -1.

**Figure 5:** Discretized clinical data for GWI compared to the two predicted diseased attractor states (SS1 [black] and SS2 [grey]).

**Figure 6**: Discretized clinical data for CFS compared to the two predicted diseased attractor states (SS1 [black] and SS2 [grey]).

**Figure 7**: Sammon projection of the hamming distances between all five states. Green dots represent the predicted model attractor states (SS0(HC), SS1, and SS2). Red dots represent the aggregated clinical data for GWI and CFS. Axes represent the aggregated ternary (-1, 0, 1) scores 1 and 2 defined such that the observed Cartesian distances between the points in 2 dimensional space is the same as the hamming distances between the points in 5 dimensional space.

**Table 1:** Ternary HIGH/LOW PASS operator

| A   B | | B | | |
|---|---|---|---|---|
| | | **-1** | **0** | **1** |
| **A** | **-1** | 0 | 0 | -1 |
| | **0** | 0 | 0 | -1 |
| | **1** | 1 | 1 | 0 |

**Table 2:** Ternary OR operator

| A   B | | B | | |
|---|---|---|---|---|
| | | **-1** | **0** | **1** |
| **A** | **-1** | -1 | 0 | 1 |
| | **0** | 0 | 0 | 1 |
| | **1** | 1 | 1 | 1 |

**Table 3:** Ternary NOT operator

| A | A |
|---|---|
| -1 | 1 |
| 0 | 0 |
| 1 | -1 |

**Table 4:** Aggregated cytokine groupings from Folcik *et al.* (2011).

| Node Title (Grouping) | Cytokines Included |
|---|---|
| MK1 | IL-12, IL-1, and IL-8 |
| MK2 | IL-10 and IL-4 |
| MK6 | IL-6 |
| MK23 | IL-23 |
| MK27 | IL-27 |
| CK1 | IFN-$\gamma$, IL-2, and TNF-$\alpha$ |
| CK2 | IL-4, IL-5, and IL-13 |

**Table 5:** Image vector equations for each node in the system shown in figure 2 including references.

| Node | Image Vector | Reference |
|---|---|---|
| MK1 | $MK(t+1) = (DC1(t))$ | Folcik *et al.* (2011) |
| MK2 (DC2) | $MK2(t+1) = (Th2(t))$ | Sia (2005) |
| MK6 | $MK6(t+1) = (DC1(t))\lozenge(TEST(t))$ | Folcik *et al.* (2011), Cutolo (2004) |
| MK23 | $MK23(t+1) = (DC1(t))$ | Folcik *et al.* (2011) |
| MK27 | $MK27(t+1) = (DC1(t))$ | Folcik *et al.* (2011) |
| CK1 | $CK1(t+1) = (NKs(t) \vee CTLs(t) \vee Th1(t))$ | Folcik *et al.* (2011) |
| CK2 | $CK2(t+1) = (Th2(t))$ | Folcik *et al.* (2011) |
| NKs | $NKs(t+1) = (MK27(t))\lozenge(CORT(t))$ | Folcik *et al.* (2011), Bush *et al.* (2012) |
| CTLs | $CTLs(t+1) = (MK1(t) \vee CK1(t) \vee TEST(t))$ | Folcik *et al.* (2011), Gonzalez *et al.* (2010) |
| Th1 | $Th1(t+1) = (MK1(t) \vee MK27(t) \vee TEST(t))\lozenge(MK2(t) \vee$ $MK6(t) \vee CK2(t) \vee CORT(t))$ | Folcik *et al.* (2011), Gonzalez *et al.* (2010), Sia (2005), Diehl and Rincon (2002), O'Garra *et al.* (2004), Liberman *et al.* (2009) |
| Th2 | $Th2(t+1) = (MK2(t) \vee MK6(t) \vee CK2(t) \vee CORT(t))\lozenge$ $(MK27(t) \vee CK1(t))$ | Folcik *et al.* (2011), Sia (2005), Liberman *et al.* (2009), Kamiya *et al.* (2011), Sia (2005) |
| DC1 | $DC1(t+1) = (MK23(t) \vee MK27(t) \vee CK1(t))\lozenge(MK2(t) \vee$ $CORT(t))$ | Folcik et al. (2011), Zen *et al.* (2011) |
| CORT | $CORT(t+1) = (MK1(t) \vee MK6(t) \vee CK1(t))\lozenge(TEST(t))$ | Cutolo (2004), Viau (2002) |
| TEST | $TEST(t+1) = \neg(CK1(t) \vee CORT(t))$ | Foster *et al.* (2003), Mehta and Josephs (2010) |

**Table 6:** Statistical significance of the one-tailed t-test performed between healthy control (HC) cytokines and hormones versus GWI cytokines and hormones. Assigned ternary values are also listed.

| Cytokine/ Hormone | Average HC Log Transform | Average GWI Log Transform | p-value | Assigned Ternary Value |
|---|---|---|---|---|
| IL-12 | 2.15 | 1.68 | 0.22 | 0 |
| IL-1a | 2.94 | 2.21 | 0.053 | -1 |
| IL-1b | 4.06 | 3.21 | 0.035 | -1 |
| IL-8 | 2.46 | 3.85 | 0.010 | 1 |
| IL-10 | 3.14 | 3.00 | 0.36 | 0 |
| IL-4 | 1.71 | 1.57 | 0.38 | 0 |
| IL-6 | 2.26 | 3.10 | 0.033 | 1 |
| IL-23 | 6.70 | 7.69 | 0.11 | 0 |
| IFN-$\gamma$ | 1.68 | 3.22 | 0.022 | 1 |
| IL-2 | 2.13 | 2.92 | 0.10 | 1 |
| TNF-$\alpha$ | 2.95 | 3.12 | 0.38 | 0 |
| IL-5 | 2.22 | 2.69 | 0.20 | 0 |
| IL-13 | 1.40 | 2.61 | 0.0022 | 1 |
| Cortisol | -3.09 | -2.58 | 0.094 | 1 |
| Testosterone | 8.81 | 8.48 | 0.033 | -1 |
| Free Testosterone | 6.07 | 5.92 | 0.17 | 0 |

**Table 7:** Statistical significance of the one-tailed t-test performed between healthy control (HC) cytokines and hormones versus CFS cytokines and hormones. Assigned ternary values are also listed.

| Cytokine/ Hormone | Average HC Log Transform | Average CFS Log Transform | p-value | Assigned Ternary Value |
|---|---|---|---|---|
| IL-12 | 2.15 | 1.96 | 0.41 | 0 |
| IL-1a | 2.94 | 2.25 | 0.19 | 0 |
| IL-1b | 4.06 | 4.01 | 0.46 | 0 |
| IL-8 | 2.46 | 3.62 | 0.067 | 1 |
| IL-10 | 3.14 | 3.60 | 0.14 | 0 |
| IL-4 | 1.71 | 2.42 | 0.26 | 0 |
| IL-6 | 2.26 | 2.12 | 0.40 | 0 |
| IL-23 | 6.70 | 8.37 | 0.029 | 1 |
| IFN-$\gamma$ | 1.68 | 2.69 | 0.22 | 0 |
| IL-2 | 2.13 | 4.26 | 0.0026 | 1 |
| TNF-$\alpha$ | 2.95 | 3.49 | 0.23 | 0 |
| IL-5 | 2.22 | 1.59 | 0.18 | 0 |
| IL-13 | 1.40 | 1.90 | 0.13 | 0 |
| Cortisol | -3.09 | -1.75 | 0.0086 | 1 |
| Testosterone | 8.81 | 8.52 | 0.074 | -1 |
| Free Testosterone | 6.07 | 5.12 | 0.033 | -1 |

**Table 8:** Average of the assigned ternary values in tables 6 and 7 within their designated model groupings for clinical data in GWI and CFS.

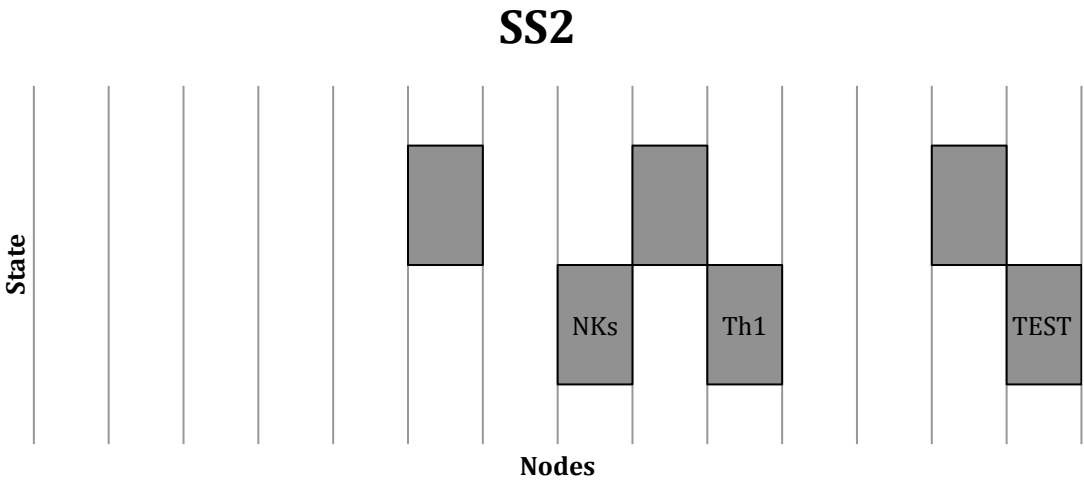| Model Cytokine/Hormone | GWI | CFS |
| --- | --- | --- |
| **MK1** | 0 | 0 |
| **MK2** | 0 | 0 |
| **MK6** | 1 | 0 |
| **MK23** | 0 | 1 |
| **CK1** | 1 | 0 |
| **CK2** | 0 | 0 |
| **CORT** | 1 | 1 |
| **TEST** | -1 | -1 |

# Figure 1

Figure 2

Figure 3

# SS1

Figure 4

# SS2



State

Nodes
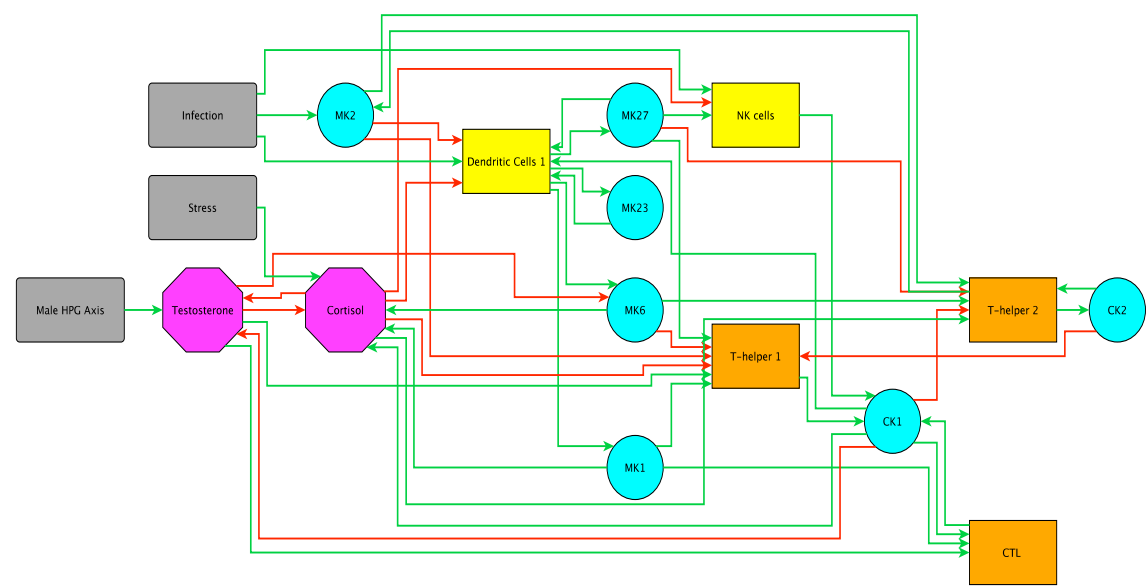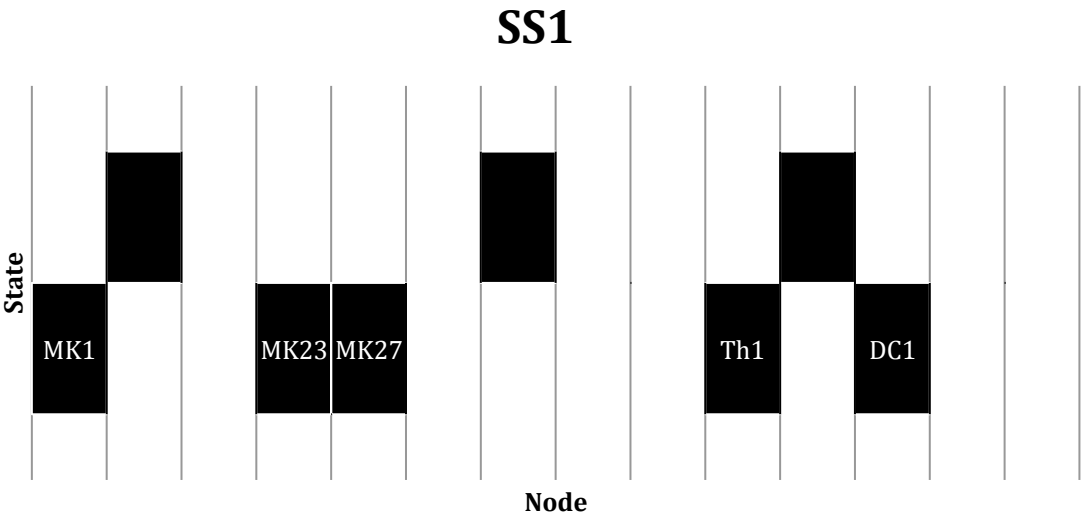
Figure 5

Figure 6

Figure 7



Sammon Projection of Ternary Hamming Distances Between States